Trends in Organic Chemistry
Vol. 19, 2018

Original Article

Structure of *O*-alkyl-*N*-ethoxycarbonyl thiocarbamate and imidothiocarbonate derivatives

Vanina M. Cayón[a], Sonia E. Torrico Vallejos[a,†], Carlos O. Della Védova[a,*], Oscar E. Piro[b], Gustavo A. Etcheverría[b] and Mauricio F. Erben[a,#]

[a]Departamento de Química, Facultad de Ciencias Exactas, Universidad Nacional de La Plata, CEQUINOR (UNLP-CONICET, CCT-La Plata and associated with CIC PBA), CC 962, Bv. 120 e/60 y 64 Nº1465 La Plata B1900, Buenos Aires; [b]Departamento de Física, Facultad de Ciencias Exactas, Universidad Nacional de La Plata and IFLP (CONICET, CCT-La Plata), CC 67, 1900 La Plata, Argentina.

ABSTRACT

O-methyl-*N*-ethoxycarbonylthiocarbamate, $CH_3CH_2OC(O)N(H)C(S)OCH_3$ (**I**), and *O*-ethyl-*N*-ethoxycarbonylthiocarbamate, $CH_3CH_2OC(O)N(H)C(S)OCH_2CH_3$ (**II**), were prepared by the addition reaction between $CH_3CH_2OC(O)NCS$ and the corresponding alcohols. Their structural and conformational properties were studied using low-temperature single crystal X-ray diffraction and vibrational spectroscopy assisted by quantum chemical calculations. Compound **I** crystallizes in the monoclinic space group $P2_1/n$ with lattice parameters a = 4.2450(1), b = 18.4992(5), c = 9.8759(3) Å, β = 95.887(3)° and 4 molecules per unit cell (Z=4), and **II** in the triclinic space group $P\bar{1}$ with parameters a = 4.1771(8), b = 9.235(2), c = 11.804(2) Å and crystallographic angles α = 98.17(1), β = 98.62(1), γ = 102.29(2)°, and Z = 2. In the crystal,the conformation around the thiocarbamate group-N(H)C(S)O- is characterized by a synperiplanar orientation of the C=S double with respect to the N-H single bond, while the methoxycarbonyl C=O double bond is in antiperiplanar orientation with respect to the N-H bond. Both species form dimers linked by NH•••S=C hydrogen bond, the N•••S non-bonding distance being 3.352(2) Å in compound **I**. Furthermore, ethoxycarbonylimidothiocarbonate species were obtained by the addition of methyl and n-butyl groups to the C=S double bond of **I** and **II**. Thus, species with formula $CH_3CH_2OC(O)N=C(SCH_3)OCH_3$ (**III**), $CH_3CH_2OC(O)N=C(SCH_3)OCH_2CH_3$ (**IV**), as well as the novel compounds $CH_3CH_2OC(O)N=C(SC_4H_9)OCH_3$ (**V**) and $CH_3CH_2OC(O)N=C(SC_4H_9)OCH_2CH_3$ (**VI**), were also prepared and fully characterized by spectroscopic methods.

KEYWORDS: carbonylthiocarbamate, sulfur chemistry, imidothiocarbonate, molecular structure, conformational properties.

1. INTRODUCTION

O-alkyl-*N*-ethoxycarbonylthiocarbamates [$C_2H_5OC(O)NHC(S)OR$] [1-3] have been extensively used as mineral flotation collectors since the introduction-almost 70 years ago- of *O*-isopropyl-*N*-ethoxycarbonylthiocarbamate (IPETC) by the Down Chemical Company. This species is efficient and selective for the flotation process of copper minerals, including sulfides. Thiocarbamates are adsorbed to sulfide minerals by donating electrons formally located on the sulfur atom lone pairs and, upon deprotonation of the NH group, promoting the

Corresponding authors: *carlosdv@quimica.unlp.edu.ar; #erben@quimica.unlp.edu.ar

†Permanent address: Centro Tecnología Agroalimentaria CTA, Universidad Mayor San Simón, Cochabamba, Bolivia.

formation of a metal-thiocarbamate complex at the mineral surface as demonstrated by Hope and Woods [4]. NMR spectra at variable temperature revealed the occurrence of conformational equilibrium of IPETC in d_8-toluene solution, the dynamic behavior being interpreted in terms of changes in the sterically confined organic backbone [5]. However, when absorbed in copper surfaces or forming a copper chloride complex, IPETC is present in a single conformation with the C=O and C=S double bonds oriented toward the metal surface.

In a previous work, we demonstrated that two *O*-alkyl-*N*-methoxycarbonylthiocarbamate species [$CH_3OC(O)NHC(S)OR$, with R= CH_3 and C_2H_5] have planar structures, with C=S and C=O double bonds of the thiocarbamate group mutually oriented toward opposite directions [6].

Thiocarbamates are susceptible to be converted into the corresponding S-alkylimidothiocarbonates by the addition of alkyl group to the nucleophilic sulfur atom of the C=S double bond [7]. Good yields and selectivity are achieved when alkyl halides are used in basic conditions. Insuasty and coworkers [8] studied the structures of two *O,S*-diethyl-*N*-(4-benzoyl)imidothiocarbonates highlighting the role of π interactions (C-H•••π and π-π stacking) in the crystal structure.

We report here the synthesis, crystal and molecular structure, and a vibrational analysis of a simple *O*-alkyl-*N*-ethoxycarbonylthiocarbamate, $C_2H_5OC(O)NHC(S)OR$, with R= $-CH_3$ (**I**), and compare these results with those already reported [1] for the closely related derivative with R=$-CH_2CH_3$ (**II**). Moreover, *S*-alkyl imidothiocarbonates -with alkyl groups including methyl (**III** and **IV**) [7] and the novel butyl derivatives (**V** and **VI**)- were prepared and their vibrational properties characterized by absorption Fourier-Transform Infrared spectroscopy (FTIR).

2. MATERIALS AND MÉTHODS

2.1. Synthesis

The procedure by Kulkarni [9] was followed for the preparation of alkoxycarbonyl isothiocyanate derivatives, by reacting ethyl chloroformate with metal thiocyanate salts in the presence of an organic solvent and basic medium given by triethyl amine, as shown in Eq. (1):

$$CH_3CH_2OC(O)Cl + KSCN \rightarrow CH_3CH_2OC(O)NCS + KCl \quad (1)$$

The $CH_2CH_3OC(O)N(H)C(S)OR$ [R= $-CH_3$ (**I**) and CH_3CH_2-(**II**)] compounds were synthesized by the addition reaction between ethoxycarbonyl isothiocyanate, $CH_3CH_2OC(O)NCS$ and the corresponding alcohol ROH, [R= $-CH_3$ (**I**) and CH_3CH_2-(**II**)] [10] according to Eq. (2):

$$CH_3CH_2OC(O)NCS + ROH \rightarrow CH_3CH_2OC(O)N(H)C(S)OR \quad (2)$$

Imidothiocarbonates can be obtained from thiocarbamates by using alkylating reagents [7]. Ethoxycarbonyl imidothiocarbonates **III-VI** were obtained according to Eq. 3 by using alkyl iodide R_1I as alkylating agent, with R_1= CH_3 (**III** and **IV**) and C_4H_9 (**V** and **VI**):

$$CH_3CH_2OC(O)N(H)C(S)OR + R_1I \rightarrow CH_3CH_2OC(O)N=C(SR_1)(OR) \quad (3)$$

2.1.1. Preparation of O-alkyl-N-ethoxycarbonyl thiocarbamates (**I** and **II**)

A freshly prepared solution of ethyl chloroformate (10 mmol) in dry acetone (50 ml) was added dropwise to a suspension of potassium thiocyanate (10 mmol) in acetone (30 ml) and the reaction mixture was refluxed for 30 minutes under nitrogen. After cooling to room temperature CH_3OH or CH_3CH_2OH (10 mmol) were added and the resulting mixture refluxed for 4 h. Ethyl acetate and water was added to the reaction mixture and the organic phase was extracted. After evaporating the solvent, a solid was obtained and recrystallized from hexane and ethyl acetate.

***O*-methyl-*N*-ethoxycarbonylthiocarbamate (I).** Mp 44(1)ºC. IR (KBr) ν/cm^{-1} 1740 (C=O), 1270 (C=S), 3258 (N-H); ^{1}H RMN ($CDCl_3$)δ= 8.49 (s, N–H broad, $^1J_{HN}$=46.32 Hz), 4.10 (s, CH_3 OC(S)-), 4.20 (q, $-CH_2-$, $^3J_{HH}$= 7.1 Hz), 1.26 (t, CH_3-, $^3J_{HH}$= 7.1 Hz, $^1J_{HC}$=63.23 Hz); ^{13}C RMN ($CDCl_3$) δ= 189.8 (C=O), 149.7 (C=S), 62.7 (C2), 59.4 (C5), 14.6 (C1). GC chromatogram (CH_2Cl_2) shows a single peak at a retention time of 5.7 min; GC-MS (EI, 70 eV) m/z [relative intensity, fragment]; 163 [30, M+], 75 [12, $CH_3OC(S)^+$], 58 [46, NCS^+], 29 [100, $CH_3CH_2^+$],

28 [19, CO^+, $C_2H_4^+$], 27 [34, $C_2H_3^+$], 15 [36, CH_3^+].

***O*-ethyl-*N*-ethoxycarbonylthiocarbamate (II).** Mp 45(1)ºC. IR (KBr) ν/cm^{-1} 1770 (C=O), 1262 (C=S), 3209 (N-H); ^{1}H RMN ($CDCl_3$) δ= 8.27 (s, N-H broad, $^1J_{HN}$=46.12 Hz), 4.61 (q, -CH_2-(CH_3CH_2O-), $^3J_{HH}$= 7.2 Hz), 4.22 (q, -CH_2- (-OCH_2 CH_3), $^3J_{HH}$= 7.1 Hz), 1.40 (t, -CH_3-(CH_3CH_2O-), $^3J_{HH}$= 7.1 Hz), 1.28 (t, -CH_3- (-OCH_2CH_3), $^3J_{HH}$= 7.1 Hz); ^{13}C RMN ($CDCl_3$) δ= 189.9 (C=O), 149.6 (C=S), 69.3 (C2), 62.7 (C5), 14.4 (C1), 13.9 (C6). GC chromatogram (CH_2Cl_2) shows a single peak at a retention time of 5.7 min; GC-MS (EI, 70 eV) m/z [relative intensity, fragment]; 177 [18, M+], 89 [7, $CH_3CH_2OCS^+$, $CH_3CH_2OC(O)NH_2$], 45 [19,$CH_3CH_2O^+$], 44 [23, CO_2^+/CS^+], 29 [100, $CH_3CH_2^+$], 28 [15, CO^+, $C_2H_4^+$], 27 [35, $C_2H_3^+$].

2.1.2. Preparation of alkoxy-carbonyl Imidothiocarbonates (III-VI). The corresponding *O*-Alkyl-*N*-ethoxycarbonylthiocarbamate (5 mmol) was dissolved in dichloromethane in a two-necked ball. Then, 1.20 mltriethylamine (5 mmol) was added and stirred for approximately 50 minutes. After that, excess iodide methyl (or butyl iodide) was added and stirred by 6 hours. The products **III-VI** turned out to be oily red-orange liquids and were isolated by successive extractions of chloroform and distilled water.

***S,O*-dimethyl-*N*-ethoxycarbonylimidothiocarbonate (III).** IR ν/cm^{-1} 1768 (C=O), 1690 (N=C), 1257 (O-C(O) -N); ^{1}H RMN ($CDCl_3$)δ= 4.26 (q, -CH_2-, $^3J_{HH}$= 7.1 Hz), 4.01 (s, -OCH_3), 2.42 (s, -SCH_3), 1.36 (t, -CH_3); ^{13}C RMN ($CDCl_3$) δ= 174.2 (C=O), 160.8 (C=S), 62.6 ($CH_3\underline{C}H_2$-), 62.3 (OCH_3), 14.4 ($\underline{C}H_3CH_2$-), 13.9 (-SCH_3). GC chromatogram (CH_2Cl_2) shows a single peak at a retention time of 6.5 min; GC-MS (EI, 70 eV) m/z [relative intensity, fragment]; 177 [19, M+], 132 [57, $C_2H_5OC(O)NCS^+$, $CH_3O(CH_3S)CNCO^+$], 58 [100, NCS^+], 29 [52, $CH_3CH_2^+$], 27 [21, $C_2H_3^+$], 15 [24, CH_3^+].

***S*-methyl-*O*-ethyl-*N*-ethoxycarbonylimidothiocarbonate (IV).** IR ν/cm^{-1} 1768 (C=O), 1690 (N=C), 1280 (O-C(O) -N); ^{1}H RMN ($CDCl_3$)δ= 4.45 (q, -CH_2O-, $^3J_{HH}$=7.1), 1.39 (t, CH_3-, $^3J_{HH}$=7.1), 4.25 (q, -OCH_2-, $^3J_{HH}$=7.1), 1.35 (t, -CH_3, $^3J_{HH}$=7.1), 2.40 (s, -SCH_3); ^{13}C RMN ($CDCl_3$)δ=173.7 (C=O), 160.9 (C=S), 66.9 ($CH_3\underline{C}H_2$-), 62.3 (-$\underline{C}H_2CH_3$), 14.3 ($\underline{C}H_3CH_2$-), 13.9 (SCH_3), 13.3 (-$CH_2\underline{C}H_3$). GC chromatogram (CH_2Cl_2) shows a single peak at a retention time of 7.0 min; GC-MS (EI, 70 eV) m/z [relative intensity, fragment]; 191 [2, M+], 118 [19, $^+NCS(CH_3)OC_2H_5$], 44 [31, CO_2^+/CS^+], 29 [100, $CH_3CH_2^+$], 27 [26, $C_2H_3^+$], 15 [2, CH_3^+].

***S*-buthyl-*O*-methyl-*N*-ethoxycarbonylimidothiocarbonate (V).** IR ν/cm^{-1} 1721 (C=O), 1693 (N=C), 1270 (O-C(O)-N); ^{1}H RMN ($CDCl_3$),δ= 4.22 (q, -CH_2O-, $^3J_{HH}$=7.1), 3.96 (s, -OCH_3, $^3J_{HH}$=7.1), 2.94 (t,-SCH_2Pr, $^3J_{HH}$=7.2), 1.62 (m,-CH_2Et), 1.42 (m,-CH_2Me), 1.33 (t,CH_3- , $^3J_{HH}$=7.1), 0.92 (t, -CH_3, $^3J_{HH}$=7.3); ^{13}C RMN ($CDCl_3$)δ= 173.2 (C=O), 160.6 (C=S), 62.3 (OCH_3), 57.4 ($CH_3\underline{C}H_2O$), 31.4 (SCH_2Pr), 30.6 (-CH_2Et), 21.8 (-CH_2Me), 14.3 ($\underline{C}H_3CH_2O$), 13.5 ($S(CH_2)_3\underline{C}H_3$). GC chromatogram ($CH_2Cl_2$) shows a single peak at a retention time of 8.2 min; GC-MS (EI, 70 eV) m/z [relative intensity, fragment]; 219 [1, M+], 118 [11, $^+NCS(CH_3)OC_2H_5$], 57 [100, $^+CH_2CH_2CH_2CH_3$, $C_2H_5OC(O)^+$], 29 [75, $CH_3CH_2^+$], 28 [14, CO^+, $C_2H_4^+$], 27 [32, $C_2H_3^+$], 15 [23, CH_3^+].

***S*-butyl-*O*-ethyl-*N*-ethoxycarbonylimidothiocarbonate (VI).** IR ν/cm^{-1} 1724 (C=O), 1696(N=C), 1233 (O-C(O)-N); ^{1}H RMN ($CDCl_3$), δ= 4.39 (q, -CH_2O, $^3J_{HH}$=7.3), 4.20(q, -OCH_2CH_3, $^3J_{HH}$=7.2), 2.91 (t,-SCH_2Pr, $^3J_{HH}$=7.0), 1.62 (m,-CH_2Et), 1.42 (m,-CH_2Me), 1.34 (t,-OCH_2CH_3, $^3J_{HH}$=7.0), 0.91 (t, -S $(CH_2)_3CH_3$, $^3J_{HH}$=7.3); 1.31 (t, CH_3-, $^3J_{HH}$=7.2); ^{13}C RMN ($CDCl_3$) δ=172.7 (C=O), 160.7 (C=S), 66.6 ($CH_3\underline{C}H_2O$), 62.2 ($O\underline{C}H_2CH_3$), 30.6 (-CH_2Et), 31.4 (SCH_2Pr), 21.8 (-CH_2Me), 14.3 ($CH_3\underline{C}H_2O$), 13.9 ($OCH_2\underline{C}H_3$), 13.5 ($S(CH_2)_3\underline{C}H_3$). GC chromatogram ($CH_2Cl_2$) shows a single peak at a retention time of 8.2 min; GC-MS (EI, 70 eV) m/z [relative intensity, fragment]; 219 [1, M+], 146 [17, $^+OCNC(SCH_3)OC_2H_5$], 57 [11, $^+CH_2CH_2CH_2CH_3$, $C_2H_5OC(O)^+$], 44 [32, CO_2^+/CS^+], 29 [100, $CH_3CH_2^+$], 15 [31, CH_3^+].

2.2. Instrumentation

2.2.1. Gas chromatography-mass spectrometry

The GC-MS measurements were recorded with a GCMS-QP2010 SHIMADZU instrument using

gaseous helium as mobile phase with the pressure in the column head equal to 100 kPa. The column used was a 19091J-433 HP-5 of 30 m x 0.32 mm x 0.25 mm film thickness. Approximately 1 μL volume of the compounds dissolved in $CHCl_3$ was chromatographed under the following conditions: the injection temperature was 200 ºC, the initial column temperature (70 ºC) was held for 2 min, then increased to 200 ºC at 10 ºC/min and held for 4 min, and finally increased to 250 ºC at 10 ºC/ min and held for 2 min. In the spectrometer the source was kept at 200 ºC.

2.2.2. X-ray diffraction data

The diffraction data of compounds **I** and **II** were collected at T = 150 K on an Oxford Xcalibur, Eos, Gemini CCD diffractometer with graphite-monochromated CuKα (λ = 1.54184 Å) radiation. X-ray diffraction intensities were measured (ω scans with ϑ- and κ-offsets), integrated and scaled with CrysAlisPro [11] suite of programs. The unit cell parameters were obtained by least-squares refinement (based on the angular settings for all collected reflections with intensities larger than seven times the standard deviation of measurement errors) using CrysAlisPro. Data were corrected empirically for absorption employing the multi-scan method implemented in CrysAlisPro. The structures were solved by direct methods with SHELXS of the SHELX suite of programs [12] and the molecular models refined with SHELXL of the same package. All hydrogen atoms were located in a difference Fourier map phased on the heavier atoms and refined at their found positions with isotropic displacement parameters. Crystal data and structure refinement results are summarized in Table 1. Full crystallographic data for both compounds were deposited with the Cambridge Crystallographic Data Centre (CCDC). Enquiries for data can be directed to: Cambridge Crystallographic Data Centre, 12 Union Road, Cambridge, UK, CB2 1EZ or (e-mail) deposit@ccdc.cam.ac.uk or (fax) +44 (0) 1223 336033. Any request to the Cambridge Crystallographic Data Centre for this material should quote the full literature citation and the reference numbers CCDC 1533226 (**I**) and CCDC 1533227 (**II**).

2.2.3. Vibrational spectroscopy

Solid and liquid-phase IR spectra were recorded with a resolution of 2 cm^{-1} in the 4000-400 cm^{-1} range on a Bruker EQUINOX 55 FTIR spectrometer.

2.2.4. NMR spectroscopy

^1H NMR, ^{13}C NMR and HSQC spectra were obtained using BrukerAvance II series 500 MHz spectrometer in $CDCl_3$. Chemical shifts are given in δ-scale (ppm).

2.2.5. Theoretical calculations

All quantum chemical calculations were performed with the GAUSSIAN 03 program package [13]. The molecular geometries were optimized to standard convergence criteria by using a density functional theory (DFT) hybrid method with Becke's non local three parameter exchange and the Lee, Young and Parr correction (B3LYP) using 6-31G(d) and 6-311++G(d,p) basis sets. The calculated vibrational properties corresponded in all cases to potential energy minima for which no imaginary frequency was found.

3. RESULTS AND DISCUSSION

3.1. Physical properties and spectroscopic characterization

Compounds **I** and **II** are solids with melting point values of 42(1) and 64(1) °C, respectively [1, 7]. The products **III-IV** are solids [7] and the compounds **V-VI** are oily orange liquid at room temperature.

Multinuclear ^1H and ^{13}C NMR spectra were measured for all these species and the results are summarized in Tables 2a and 2b for the ^1H and ^{13}C NMR spectra, respectively. These assignments are clearly supported by HSQC (heteronuclear single quantum coherence) 2D-NMR spectroscopy as shown in the Supplementary Information' section (Figures S1a,b) for the novel species **V-VI**. The spectrum shows a peak for each unique proton attached to the carbon atom being considered. Therefore, this analysis confirms the molecular structure.

GC chromatogram shows single peaks at retention times 5.7, 6.3, 6.5, 7.0, 8.2, and 8.6 minutes for molecules **I-VI**, respectively. The studied

Table 1. Crystal data and structure refinement results for $C_2H_5OC(O)N(H)C(S)OCH_3$ (**I**) and $CH_3CH_2OC(O)N(H)C(S)OCH_2CH_3$ (**II**).

	(**I**)	(**II**)
Empirical formula	$C_5H_9NO_3S$	$C_6H_{11}NO_3S$
Formula weight	163.19	
Temperature (K)	150(2)	150(2)
Wavelength (Å)	1.54184	1.54184
Crystal system	Monoclinic	Triclinic
Space group	$P2_1/n$	P-1
Unit cell dimensions		
a (Å)	4.2450(1)	4.1771(8)
b (Å)	18.4992(5)	9.235(2)
c (Å)	9.8759(3)	11.804(2)
α (º)	90.0	98.17(1)
β (ª)	95.887(3)	98.62(1)
γ (º)	90.0	102.29(2)
Volume (Å3)	771.46(4)	432.7(1)
Z, density (calculated, Mg/m3)	4, 1.405	2, 1.360
Absorption coefficient (mm-1)	3.376	3.052
F(000)	344	188
Crystal size (mm3)	0.553 x 0.235 x 0.059	0.214 x 0.205 x 0.162
θ-range for data collection (º)	4.781 to 71.988	3.851 to 71.899
Index ranges	-5≤h≤ 4, -18≤k≤22, -11≤l≤11	-5≤h≤5, -5≤k≤11, -14≤l≤13
Reflections collected	2711	2722
Independent reflections	1503 [R(int) = 0.0248]	1665 [R(int) = 0.0409]
Observed reflections [I>2σ(I)]	1320	1266
Completeness (%)	100.0 (to θ = 67.684°)	99.7 % (to θ = 67.684°)
Refinement method	Full-matrix least-squares on F^2	Full-matrix least-squares on F^2
Data / restraints / parameters	1503 / 0 / 127	1665 / 0 / 144
Goodness-of-fit on F2	1.053	1.044
Final R indicesa [I>2σ(I)]	R1 = 0.0431, wR2 = 0.1183	R1 = 0.0504, wR2 = 0.1342
R indices (all data)	R1 = 0.0481, wR2 = 0.1241	R1 = 0.0696, wR2 = 0.1573
Largest diff. peak and hole (e.Å-3)	0.376 and -0.322	0.499 and -0.390

[a] $R_1=\Sigma||F_o|-|F_c||/\Sigma|F_o|$, $wR_2=[\Sigma w(|F_o|^2-|F_c|^2)^2/\Sigma w(|F_o|^2)^2]^{1/2}$

compounds show the parent ion (M^+) peaks at m/z= 163, 177, 177, 191, 219 and 233 with intensities 30, 18, 19, 1, 2, and 2% for **I-VI**, respectively. The mass spectra were assigned to expected ionic fragments from logical ruptures of the corresponding M+ molecular ions as shown in Table 3.

The electron impact fragmentation of thiocarbamate compounds is dominated by the formation of characteristic carbamothioic *S*-acids and amide species, as studied by Martínez-Álvarez *et al*. [10]. For example, as shown in the Scheme 1 for **II**, the O-alkylcarbamothioic *S*-acid intermediate at m/z = 149 is formed *via* elimination of the

Table 2a. ^{1}H NMR chemical shifts (δ) and coupling constants (Hz) for **I-VI** molecules.

H	I	II	III	IV	V	VI
NH	8.49 *s*(46.32)	8.27 *s*(46.12)	-	-	-	-
Me$\underline{CH_2}$O	4.20 *m*(7.1)	4.61 *q*(7.2)	4.26 *q*(7.1)	4.45 *q*(7.1)	4.22 *q*(7.1)	4.39 *q*(7.3)
$\underline{Me}CH_2O$	1.26 *t*(7.1)	1.40 *t*(7.1)	1.36 *t*(7.1)	1.39 *t*(7.1)	1.33 *t*(7.1)	1.31 *t*(7.2)
OCH_3	4.10 *s*	-	4.01 *s*	-	3.96 *s*(7.1)	-
O$\underline{CH_2}$Me	-	4.22 *q*(7.1)	-	4.25 *q*(7.1)	-	4.20 *q*(7.2)
$OCH_2\underline{Me}$	-	1.28 *t*(7.1)	-	1.35 *t*(7.1)	-	1.34 *t*(7.0)
SCH_3	-	-	2.42 *s*	2.40 *s*	-	-
SCH_2Pr	-	-	-	-	2.94 *t*(7.2)	2.91 *t*(7.0)
$SCH_2\underline{CH_2}Et$	-	-	-	-	1.62 *m*	1.62 *m*(7.6)
$S(CH_2)_2\underline{CH_2}Me$	-	-	-	-	1.42 *m*	1.42 *m*(7.5)
$S(CH_2)_3\underline{Me}$	-	-	-	-	0.92 *t*(7.3)	0.91 *t*(7.3)

Table 2b. ^{13}C NMR chemical shifts for **I-VI** molecules.

C	I	II	III	IV	V	VI
C=O	189.8	190.0	174.2	173.7	173.2	172.7
C=S	149.4	149.2	160.7	160.9	160.6	160.7
Me$\underline{CH_2}$O	62.8	69.3	62.5	66.9	57.4	66.6
$\underline{Me}CH_2O$	14.4	14.4	14.3	14.3	14.3	14.3
OCH_3	59.4	-	62.3	-	62.3	-
O$\underline{CH_2}$Me	-	62.7	-	62.3	-	62.2
$OCH_2\underline{Me}$	-	13.9	-	13.3	-	13.9
SCH_3	-	-	13.9	13.9	-	-
SCH_2Pr	-	-	-	-	31.3	31.4
$SCH_2\underline{CH_2}Et$	-	-	-	-	30.5	30.6
$S(CH_2)_2\underline{CH_2}Me$	-	-	-	-	21.8	21.8
$S(CH_2)_3\underline{Me}$	-	-	-	-	13.5	13.5

olefin corresponding to the alkoxy group (OCH_2CH_3) after hydrogen rearrangement. The second fragmentation step involves a new hydrogen rearrangement, followed by the elimination of carbonyl sulfide (OCS) to form the amide, observed at m/z = 89.

Additional evidences for identifying the synthesized compounds **I** and **II** come from the analysis of their IR spectra. The characteristic absorption for the NH group appears as a broad band at 3258 and 3209 cm^{-1} for the υ(NH) stretching vibration mode while the deformation mode δ(NH) is observed as intense bands at 1514 y 1536 cm^{-1}, for compounds **I** and **II**, respectively. The C=O stretching modes are observed as very strong signals at 1742 and 1770 cm^{-1} and the υ(C=S) stretching vibrations can be assigned for **I** and **II** as medium intensity absorptions at 1255 y 1262 cm^{-1}.

The spectra of compounds **III-VI** are dominated by strong bands in the region of 1700 cm^{-1} overlapped with the carbonyl signal and assigned

Table 3. Main peaks observed in the mass spectra (70 eV electron ionization) for **I-VI** species.

m/z			Intensity (%)				Fragments
	I	**II**	**III**	**IV**	**V**	**VI**	
15	36	-	24	3	23	31	CH_3^+
27	34	35	21	26	32	-	$C_2H_3^+$
28	19	15	7	6	14	-	CO^+, $C_2H_4^+$
29	100	100	52	100	75	100	$CH_3CH_2^+$
31	7	7	-	-	-	-	CH_3O^+
44	26	23	-	31	-	32	CO_2^+/CS^+
45	-	19	-	-	-	-	$CH_3CH_2O^+$
57	-	-	-	2	100	11	$CH_2CH_2CH_2CH_3^+$, $C_2H_5OC(O)^+$
58	43	-	100	-	-	-	NCS^+
75	12	-	-	-	-	-	$CH_3OC(S)^+$
89	1	7	-	-	-	-	$CH_3CH_2OCS^+$, $CH_3CH_2OC(O)NH_2^+$
118	-	-	-	19	11	-	$NCS(CH_3)OC_2H_5^+$
119	6	-	-	-	-	-	$CH_3OC(S)N(H)C(O)H^+$
132	-	-	57	-	-	-	$C_2H_5OC(O)NCS^+$, $CH_3O(CH_3S)CNCO^+$
146	-	-	-	-	-	17	$^+OCNC(SCH_3)OC_2H_5$
149	-	4	-	-	-	-	$CH_3CH_2OC(O)N(H)C(O)SH^+$
163	30	-	-	-	-	-	$[CH_3CH_2OC(O)N(H)C(S)OCH_3]\cdot^+$
177	-	18	19	-	-	-	$[CH_3CH_2OC(O)N(H)C(S)OCH_2CH_3]\cdot^+$, $[CH_3CH_2OC(O)N=C(SCH_3)OCH_3]\cdot^+$
191	-	-	-	1	-	-	$[CH_3CH_2OC(O)N=C(SCH_3)OCH_2CH_3]\cdot^+$
219	-	-	-	-	2	-	$[CH_3CH_2OC(O)N=C(SC_4H_9)OCH_3]\cdot^+$
233	-	-	-	-	-	2	$[CH_3CH_2OC(O)N=C(SC_4H_9)OCH_2CH_3]\cdot^+$

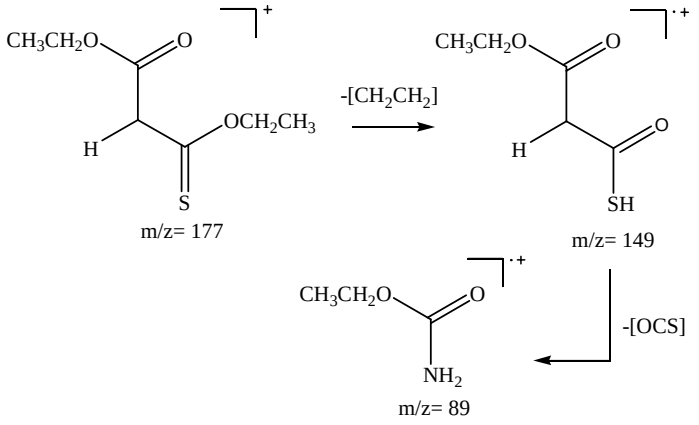

Scheme 1. Fragmentation pathways of alkylthiocarbamates under EI conditions.

to the υ(C=N) stretching mode. Finally, new bands appear in the region around 3000 cm^{-1} denoting the presence of the alkyl groups in the synthesized compounds. A detailed vibrational analysis is given below.

3.2. Quantum chemical calculations

To analyze the conformational preferences of the compounds studied in the present work, the potential energy functions for internal rotation around the δ(C1C2-O1C3) and δ(C3N1-C4O3) dihedral angles were calculated at the B3LYP/6-31G(d) level by allowing geometry optimizations with the respective dihedral angles (δ) varying from 0° to 360° in steps of 10°. The potential energy functions for compounds **I** and **II** are shown in Figures 1A and B (see Figure 2 for atoms numbering).

For the specie **I**, the curve obtained for the δ (C1C2-O1C3) dihedral angle (Figure 1A) indicates the presence of two minima; the most stable conformation corresponds to the *anti-syn-syn-anti-syn* (*a-s-s-a-s*) conformer and the second one to the *gauche*(+)-*syn-syn-anti-syn* (+*g-s-s-a-s*) form. Thus, we describe "*a-s-s-a-s*" conformer as the mutual orientation around the C2-O1, O1-C3, C3-N1, N1-C4 and C4-O3 single bonds. For the "+*g-s-s-a-s*" conformer, ethyl group is out of molecular plane and it is located slightly higher in energy by 0.40 kcal mol^{-1}. This form corresponds to a conformer with *gauche* orientation of the δ(C1C2-O1C3) dihedral angle.

The curve obtained as a function of the dihedral angle around the N1-C4 (Figure 1B) bond shows a minimum at δ(C3N1-C4O3)= 0°, corresponding to the *anti-syn-syn-anti-syn* conformer and the second stable form corresponding to the *anti-syn-syn-syn-syn* conformer.

For the specie **II**, the curve obtained (Figure 1A) for the δ(C1C2-O1C3) dihedral angle also shows two minima, the most stable conformations correspond to *anti-syn-syn-anti-syn-anti* (mutual orientation around the C2-O1, O1-C3, C3-N1, N1-C4, C4-O3 and O3-C5 single bonds and *gauche*(-)-*syn-syn-anti-syn-anti* (*gauche* orientation of the C1-C2 bond with respect to O1-C3 bond) forms. The second stable conformer is located 0.87 kcal mol^{-1} energy above the minimum. Finally, the curve obtained as a function of the δ(C3N1-C4O3) dihedral angle (Figure 1B) shows two minimum corresponding to the *anti-syn-syn-anti-syn-anti* and *anti-syn-syn-syn-syn-anti* conformers, in increasing order of energy.

Additionally, full geometry optimizations and frequency calculations were computed for each of the most stable structures of both compounds by using the B3LYP method and the more extended 6-311++G(d,p) basis sets. The optimized structure for the conformers are shown in Figure 2 and

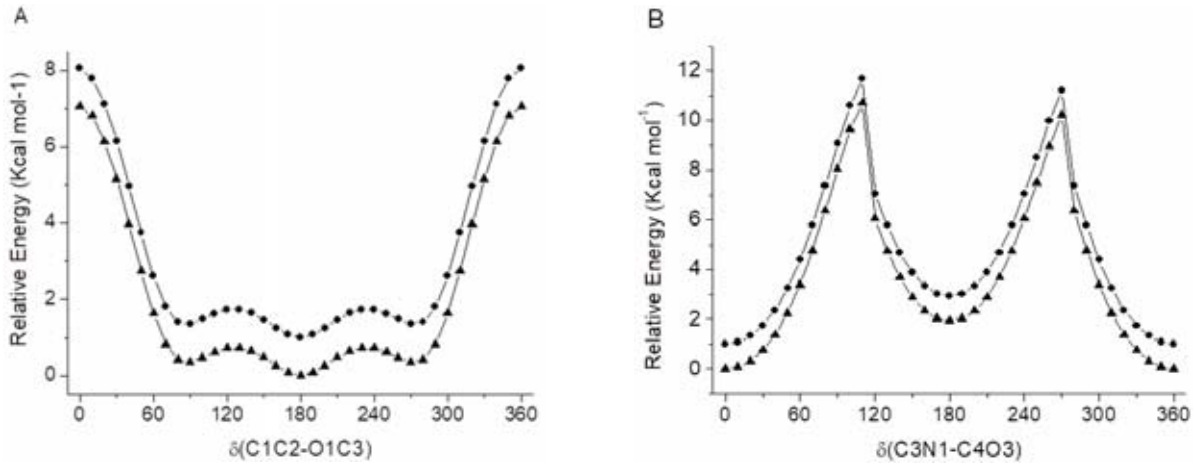

Figure 1. Calculated [B3LYP/6-31G(d)] potential energy function for internal rotation of $CH_3CH_2OC(O)N(H)C(S)OR$, R= CH_3 (compound **I**, triangle line) and R= CH_2CH_3 (compound **II**, point line) as a function of the δ(C1C2-O1C3) (**A**) and δ(C3N1-C4O3) (**B**). The curve corresponding to the compound II was up-shifted by 1 kcal mol^{-1} in energy.

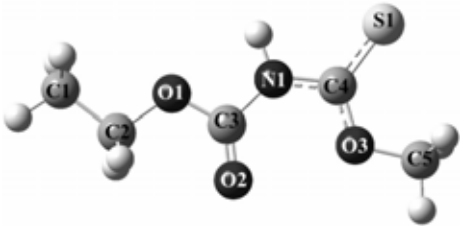

anti-syn-syn-anti-syn
(*0.00*)

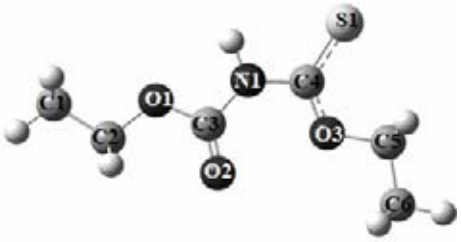

anti-syn-syn-anti-syn-anti
(*0.00*)

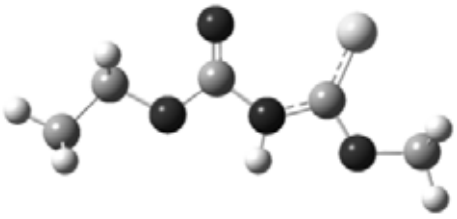

anti-syn-syn-syn-syn
(*1.58*)

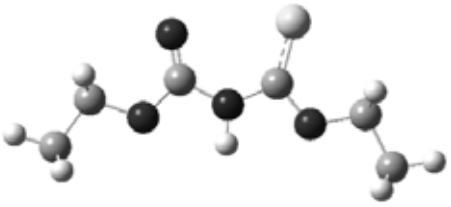

anti-syn-syn-syn-syn-anti
(*1.89*)

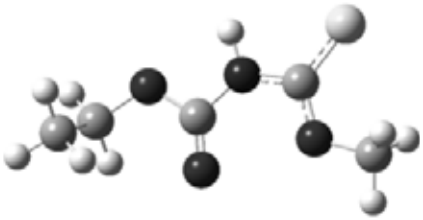

gauche(+)-*syn-syn-anti-syn*
(*0.40*)

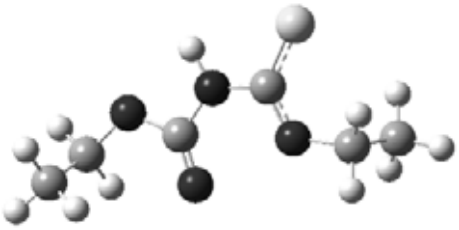

gauche(+)-*syn-syn-anti-syn-gauche*(-)
(*1.28*)

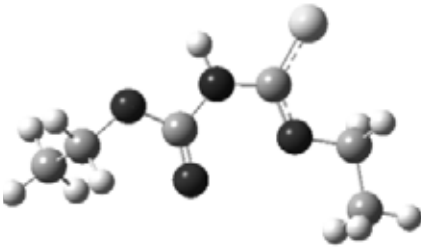

gauche(-)-*syn-syn-anti-syn-gauche*(-)
(*1.31*)

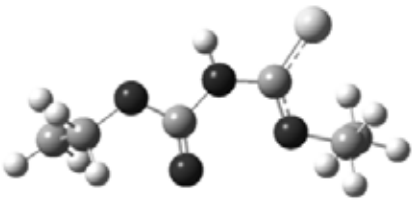

gauche(-)-*syn-syn-anti-syn-anti*
(*0.87*)

Figure 2. Optimized molecular structures at the B3LYP/6-311++G(d,p) level of approximation -with atom numbering- of the main conformers of *O*-methyl-*N*-ethoxycarbonylthiocarbamate (**I**) (left side) and *O*-ethyl-*N*-ethoxycarbonylthiocarbamate (**II**) (right side) with computed relative energy.

predicted relative energies, ΔE° (corrected by zero-point energy), are given within parenthesis.

3.3. Vibrational analysis

3.3.1. N-ethoxycarbonyl-O-alkyl thiocarbamates

To our knowledge, neither experimental nor theoretical vibration analysis for $CH_3CH_2OC(O)N(H)C(S)OR$ (R = CH_3- and CH_3CH_2-) have so far been performed. The IR spectra of compounds **I** and **II** in the solid phase are shown in Figure 3(a) and 3(b), respectively. Experimental and calculated [B3LYP/6-311++G(d,p)] frequencies and intensities are given in the Supplementary Information' section (Table S1a and S1b). A tentative assignment of the observed bands was carried out by comparison with spectra of related molecules [14-23]. The gas-phase molecular symmetry for the more stable conformations is C_S for both compounds and therefore all 51 (31A' + 20A") and 60 (34A' + 26A") normal modes for **I** and **II**, respectively, are active in the IR and Raman spectra. The general features of the vibration spectra of solid $CH_3CH_2OC(O)NHC(S)OR$ (R = CH_3- and CH_3CH_2-) can be explained by supposing the sole presence of the most stable *a-s-s-a-s* and *a-s-s-a-s-a* conformers, respectively. The assignment of the characteristic vibration modes of the main -OC(O)NHC(S)O- moiety is summarized in Table 4.

Strong and very strong bands at 3258 cm^{-1} for **I** and at 3209 cm^{-1} for **II** can be assigned in the IR spectra to the N-H stretching vibrational mode. These values agree with the corresponding ones in the IR spectrum of O-ethyl benzoyl thiocarbamate [14] and with the similar molecules $CH_3OC(O)N(H)C(S)OR$ (R = CH_3-, CH_3CH_2-) [6], where this mode is observed in the region of 3200 cm^{-1}. The very strong bands at 1742 and 1770 cm^{-1}, were assigned to the C=O modes, respectively.

The IR absorptions observed at 1270 and 1262 cm^{-1} were assigned to the ν(C=S) mode for compounds **I** and **II**, respectively, in good agreement with the calculated values (Supplementary Information, Tables S1a, b). The formation of C=S•••H-X intermolecular hydrogen bonds seems to strongly effect the frequency of the ν(C=S) mode. For example, a strong band at 1203 cm^{-1} was observed in the IR spectra of (E)-O-ethyl-N-(4-chlorophenyl)thiocarbamate, a molecule which presents intermolecular hydrogen bonds [16], while the ν(C=S) stretching frequency for some free thioureas are reported in the region around 1325 cm^{-1} [18]. The relatively low frequency values for the ν(C=S) stretching mode observed in the IR spectra of the title compounds can be related to the formation of intermolecular hydrogen bonds involving the thiocarbonyl group. Indeed, N-H•••S=C bonds are observed in the

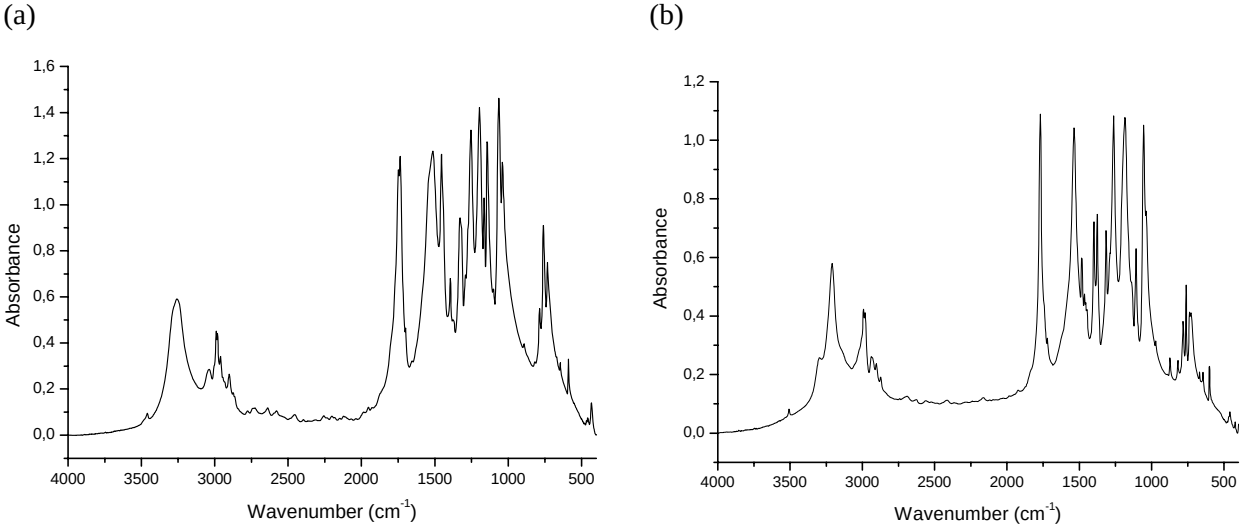

Figure 3. Solid IR (in KBr pellet) for (a) $CH_3CH_2OC(O)N(H)C(S)OCH_3$ (**I**) and (b) $CH_3CH_2OC(O)N(H)C(S)OCH_2CH_3$ (**II**).

Table 4. Experimental and theoretical [B3LYP/6-311++G(d,p)] vibration frequencies (cm^{-1}) and band intensities and mode assignments for the -OC(O)N(H)C(S)O- moiety of *O*-methyl- (**I**) and *O*-ethyl- (**II**) *N*-ethoxycarbonylthiocarbamates.

Experimental[a]		Calculated[a]		
I	**II**	**I**	**II**	**Assignment**
3258s	3209vs	3623(10)	3621(9)	ν(NH)
1742vs	1770vs	1823(59)	1822(53)	ν(C=O)
1514vs	1536vs	1540(100)	1536(88)	δ(NH)
1317s	1314s	1348(48)	1331(47)	ν_{as}(N-C(S))
1270m	1262m	1264(51)	1261(53)	ν(C=S)
762s	738m	771(4)	770(3)	δoop(ONOC)
589w	646w	634(<1)	633(<1)	δoop(SNOC)

[a]Band intensity; vs: very strong; s: strong; m: medium; Calculated: within parentheses (in Km/mol).

X-ray crystal structure of compounds **I** and **II** [19], as will be discussed in the next section.

In connection with the amide- and thioamide-like groups, very strong IR absorptions at 1514 and 1536 cm^{-1} for the **I** and **II**, respectively, are assigned to the in-plane N-H deformation mode [δ(NH), A']. Strong IR absorptions at 1317 and 1314 cm^{-1} are assigned to the N-C(S) stretching mode for **I** and **II**, respectively. On the other hand, strong IR absorptions at 1328 and 1314 cm^{-1} are assigned to the N-C(O) stretching mode of the *O*-methyl- and *O*-ethyl-*N*-ethoxycarbonylthiocarbamate, in agreement with reported data for related species [11-14, 16-18].

Other clearly defined bands in the IR spectra correspond to the C=O and N-H out-of-plane deformation modes observed at 762 and 738 cm^{-1}, for **I** and **II**, respectively. The corresponding IR absorptions due to C=S out-of-plane deformation mode are observed at 589 and 646 cm^{-1} for compounds **I** and **II**, respectively.

3.3.2. Ethoxycarbonyl imidothiocarbonates

Selected vibrational frequencies for **III-VI** molecules calculated by the B3LYP/6-311++G (d,p) method compared with experimental values from the IR spectrum in liquid phase are given in Table 5. The main vibrational features of the -OC(O)N=C(S-R)O- moiety, where R= $-CH_3$ (**III** and **IV**) and $-C_4H_9$ (**V** and **VI**) groups will be discussed. Comparing the IR spectrum of structures **I** and **II** with the spectra obtained for species **III-VI**, the absence of some bands can be noticed, as those assigned to the ν(NH) and ν(C=S) stretching modes due to the formation of the new N=C bond and alkyl substitution at the sulfur atom.

Intense bands appearing near 1700 cm^{-1}correspond to the N=C stretching for **III-VI** molecules. New bands are also observed in the region of 800 cm^{-1} of the spectrum, assigned to the characteristic ν(S-C) stretching of the S-R group.

The substitution of imidothiocarbonate with OCH_3 groups and $-OCH_2CH_3$ groups has a smaller effect on the vibrational properties of molecules **III-VI**, the most salient feature being associated with an intense absorption at 1050 cm^{-1} corresponding to the ν(O-C) stretching mode.

3.4. X-ray diffraction analysis

ORTEP [24] drawings of **I** and **II** solid state molecules are shown in Figure 4. Both substances are arranged in the crystal as centro-symmetric dimeric units where the molecules interact *via* N-H•••S=C hydrogen bonds [H…S distances of 2.53(3) Å and 2.57(5) Å and N-H…S angles of 170(3)º and 172(4)º for **I** and **II**, respectively]. In Table 6 the main geometric parameters derived from the structure refinement are given, along with the corresponding values obtained from quantum chemical calculations.

Table 5. Main experimental and theoretical [B3LYP/6-311++G(d,p)] frequencies (cm^{-1}) for **III-VI** species.

$C_2H_5OC(O)NCSR_1OR_2$[a]								
III		**IV**		**V**		**VI**		
Calc[b]	Exp[c]	Calc	Exp	Calc	Exp	Calc	Exp	Assignment
1771(49)	1768s[d]	1770(41)	1768s	1770(51)	1721m	1768(42)	1724s	ν(C=O)
1712(98)	1690vs	1708(83)	1690s	1708(100)	1693s	1704(83)	1696s	ν(N=C)
1257(100)	1257s	1254(100)	1280vs	1253(83)	1270vs	1252(100)	1233s	ν_{as}(O-C(O)-N)
1052(32)	1061vs	1048(26)	1096s	1050(38)	1059s	-	-	ν(O-CH_3)
-	-	1061(8)	1062s	1061(7)	1060s	1062(9)	1062s	ν_{as}(O-CH_2-CH_3)
716(<1)	799s	712(<1)	796w	716(5)	800s	714(3)	798s	ν(S-C)

[a]General formula for **III-VI**, where R_1 = CH_3, C_4H_9 and R_2 = CH_3, C_2H_5; [b]Calculated frequencies; [c]Experimental frequencies (cm^{-1}); [d]Band intensity; vs: very strong; s: strong; m: medium.

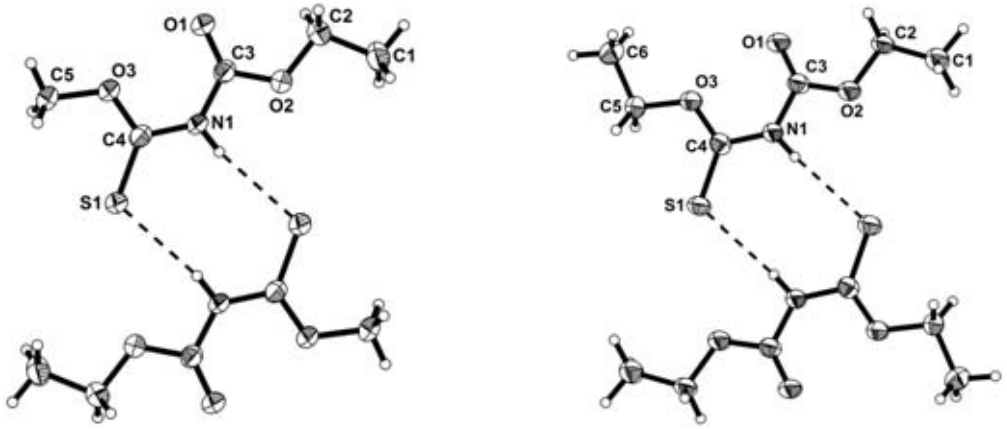

Figure 4. View of dimeric $CH_3CH_2OC(O)N(H)C(S)OCH_3$ (**I**) in the solid state showing the labeling of the atoms and their displacement ellipsoids at the 50% probability level. The unlabeled monomer is related to the labeled one by a crystallographic inversion center of the monoclinic $P2_1/n$ space group. H-bonds are indicated by dashed lines. View of dimeric $CH_3CH_2OC(O)N(H)C(S)OCH_2CH_3$ (**II**). The unlabeled monomer is related to the labeled one by a crystallographic inversion center of the triclinic $P\bar{1}$ space group.

The C-N bond length is shorter than the average value of 1.472(5) [25] Å. In the thiourea group (S)C-NH [N-C4 = 1.359(3) Å] C-N bond is considerably shorter than the amide bond (O)C-NH[N-C3 = 1.392(3) Å]. This trend seems to be characteristic for thiocarbamate compounds [14, 16, 19, 26]. However, for carboxyl-substituted thioureas the above trend is the opposite, i.e., the C-N bond in the amidic-like group (O=C-NH-) is shorter than the C-N thiourea bond (S)C-NH [15, 17, 24, 25]. The C=O double bond [1.200(2)Å] is very well reproduced by quantum chemical calculations (1.200 Å) and similar to that reported for O-ethyl benzoylthiocarbamate (1.205(3) Å)[7, 9].

Differences in the (O)C-O and (S)C-O single-bond lengths for the methoxy and ethoxy groups for **I** (1.335(2) and 1.320(2) Å for the O1-C3 and C4-O3 bonds, respectively) suggest that resonance interactions are extended over the whole planar structure.

Table 6. Experimental and calculated [B3LYP/6-311++G(d,p)] selected geometric parameters for the most stable conformers of $CH_3CH_2OC(O)N(H)C(S)OR$ (R = CH_3- and CH_3CH_2-).

Parameter	$CH_3CH_2OC(O)N(H)C(S)OCH_3$ (I)		$CH_3CH_2OC(O)N(H)C(S)OCH_2CH_3$ (II)	
	Experimental X-ray	Calculated[a]	Experimental X-ray	Calculated[a]
C1-C2	1.499(3)	1.514	1.505(5)	1.514
C2-O1	1.453(2)	1.451	1.457(4)	1.450
O1-C3	1.335(2)	1.353	1.338(4)	1.353
C=O	1.200(2)	1.200	1.203(4)	1.200
N1-C3	1.392(3)	1.399	1.397(4)	1.398
N1-C4	1.359(3)	1.381	1.367(4)	1.382
C=S	1.657(2)	1.659	1.653(3)	1.662
C4-O3	1.320(2)	1.320	1.321(4)	1.318
C5-O3	1.449(3)	1.438	1.453(4)	1.452
C5-C6	-	-	1.507(5)	1.514
C3-N1-C4	129.3(2)	130.1	128.4(3)	130.1
O2-C3-N1	127.3(2)	127.6	126.0(3)	127.7
N1-C4-S1	121.4(1)	120.9	121.6(2)	120.2
S1-C4-O3	125.5(2)	126.7	126.3(2)	127.6
C4-O3-C5	117.5(2)	119.3	118.1(2)	120.8
O3-C5-C6	-	-	106.7(3)	106.9
δ(C5O3-C=S)	3.2(3)	0.0	5.34(4)	0.0
δ(C3N-C=S)	-177.7(2)	-179.9	-168.6(3)	-179.9
δ(C2O1-C=O)	7.3(3)	0.0	4.1(5)	0.0
δ(C4N-C=O)	11.0(4)	0.0	1.9(6)	0.0
δ(C1C2-O1C3)	167.7(2)	179.9	-177.2(3)	179.9
δ(NC4-O3C5)	-177.9(2)	-180.0	-175.1(3)	179.9
δ(C4O3-C5C6)	1.500(3)	-	-178.7(3)	-179.9

[a] *anti-syn-syn-anti-syn* and *anti-syn-syn-anti-syn-anti* conformers for **I** and **II**, respectively.

Only *anti-syn-syn-anti-syn* and *anti-syn-syn-anti-syn-anti* conformations are found in the crystal for **I** and **II**, respectively. The trans orientation of sulfur and oxygen donor atoms within the -C(O)NHC(S)- moiety has a significant role on the molecular packing of the compounds. These conformations are stabilized in the crystal by the intermolecular interaction of N-H•••S=C hydrogen bonds [d(N•••S) = 3.352(2)Å for **I**] between adjacent molecules forming dimers of $R_2^2(8)$ motif (see Figure 4). This type of hydrogen-bond formation represents an example

Table 7. Comparison of the C=S bond length in compounds with and without intermolecular N-H•••S=C hydrogen bonds.

Species	Main moiety	C=S distance (Å)	Reference
$CH_3CH_2OC(O)N(H)C(S)OCH_3$	-C(O)N(H)C=SO-	1.657(19)[a]	This work
$CH_3CH_2OC(O)N(H)C(S)OCH_2CH_3$	-C(O)N(H)C=SO-	1.654(2)[a]	This work,[19]
$CH_3CH_2OC(S)N(H)C(O)OCH_3$	-C(O)N(H)C=SO-	1.654(2)[a]	[6]
$CH_3CH_2OC(S)N(H)C_6H_4Cl$	-C(O)N(H)C=SO-	1.667(2)[b]	[16]
$ClC_6H_4N(H)C(S)N(H)C(O)C_6H_4CH_3$	-C(O)N(H)C=SN-	1.6696(18)[b]	[29]
$[(C_2H_5)_2NC(S)N(H)C(O)]_2(CH_2)_3$	-C(O)N(H)C=SN-	1.687(3)[b]	[30]
$(C_2H_5)_2NC(S)N(H)C(O)C_6H_4OCH_3$	-C(O)N(H)C=SN-	1.676(4)[b]	[31]
$CH_3CH_2OC(S)N(H)C(O)C_6H_5$	-C(O)N(H)C=SO-	1.619(3)[c]	[14]
$[C_2H_5OC(S)N(H)C(O)]_2$-1,4C_6H_4	-C(O)N(H)C=SO-	1.638(3)[c]	[32]
$(CH(CH_3)_2)OC(S)N(H)C(O)C_4OH_4$	-C(O)N(H)C=SO-	1.636(5)[c]	[33]
$[CH_3OC(S)N(H)C(O)]_2$-1,3C_6H_4	-C(O)N(H)C=SO-	1.637(2)[c]	[34]

[a]Experimental results; [b]Related compounds having N-H…S=C hydrogen bonds; [c]Related compounds which do not present NH…S=C hydrogen bonds.

of π-bond cooperative behavior, frequently called 'Resonance-Assisted Hydrogen Bonding (RAHB)' [27], which occurs when XH groups are polarized by charge flow through π-bonds. As a result of the dual donor and acceptor capacity of the thioamide unit, intermolecular N-H•••S=C hydrogen bonds are common in thiourea compounds. The presence of this type of interaction strongly affects the C=S bond length, which is noticeably lengthened [d(C=S) = 1.657(2) Å for **I**]. The comparison of the C=S bond length for a series of molecules possessing the -C(O)N(H)C(S)- moiety is shown in Table 7. Species displaying N-H•••S-C hydrogen bonds have longer C=S bond lengths by ca. 0.04 Å than similar species without intermolecular N-H•••S=C interactions.

Previous X-ray diffraction analysis carried out for related *O*-alkyl-*N*-methoxycarbonylthiocarbamates species show concordance with these experimental results. For example, intermolecular d(N•••S) distances for *O*-ethyl-*N*-methoxycarbonyl [4], *O*-ethyl-*N*-ethoxycarbonyl [19] and (E)-*O*-Ethyl-*N*-(4-nitrophenyl) thiocarbamates [28] are 3.387(1), 3.388(2) and 3.444(2) Å, respectively.

Interestingly, X-ray diffraction analysis carried out for the closely related *O*-ethyl-*N*-benzoylthiocarbamate species [14] shows that the crystal packing is dominated by endless chains linked by N-H•••O=C hydrogen bond interactions [35]. The N-H•••S=C intermolecular interactions are absent in the crystal, and the *syn-syn-syn* conformation is the only form observed. Moreover, theoretical studies predict the *syn-anti-syn* form as the most stable conformer of this molecule isolated in a vacuum.

Previous structural features can be rationalized considering that several resonant structures are feasible for the thiocarbamate central moiety. Three of them are showed in Scheme 2. It is well known that the traditional picture of amide resonance is more appropriate for thioamides than for oxoamides. Moreover, previous studies for $H_2N(C=X)H$ species showed that amide resonance increases with a decrease in the electro-negativity of X (X=O, S, Se) [1]. By using *ab initio* molecular orbital calculations, Wiberg and Rablen [36] concluded that amide resonance is dependent on the charge polarization across the C=X double bond; the charge polarization across thiocarbonyl bond is weaker than that in C=O bond, and hence the contribution from resonance structure is much more reduced for the oxygen analogs. In perfect

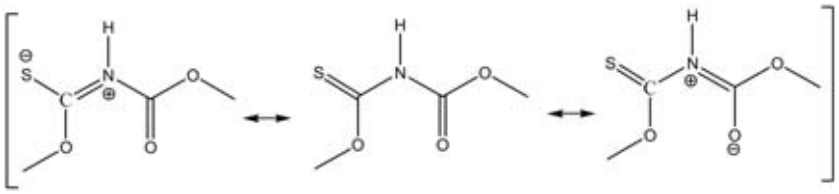

Scheme 2. Main resonance structure for the central thiocarbamate moiety.

agreement with these results, vibration and structural data for compound **I** are consistent with a larger π resonant contribution of the thioamide group (structure III) when comparing with the amide group structure (structure II).

4. CONCLUSIONS

Two *O*-alkyl-*N*-ethoxycarbonylthiocabamates were prepared in high yield and purity by treating $CH_3CH_2OC(O)NCS$ with the corresponding alcohols in mild conditions. Conformational and structural properties were determined by using experimental techniques which include vibrational spectroscopy (IR) as well as X-ray diffraction analysis. For both substances, it was determined that the molecular skeleton is essentially planar. Results derived from the quantum chemical calculations show that the central -OC(O)N(H) C(S)- moiety adopts a planar structure with a preferred *anti-syn* orientation around the C3-N and N-C4 single bonds. These forms are present in crystalline $CH_3CH_2OC(O)N(H)C(S)OCH_3$ and $CH_3CH_2OC(O)N(H)C(S)OCH_2CH_3$ [19] as centro-symmetric dimeric units held by resonance-assisted N-H•••S=C hydrogen bonds.

Synthesis, characterization and a complete vibrational study of imidothiocarbonate compounds were achieved successfully. These were obtained by alkylation of the sulfur atom in the thiocarbamate group of species **I** and **II** with alkyl iodides in basic medium. Molecules with formula $C_2H_5OC(O)N=CS(CH_3)OR$ and $C_2H_5OC(O)N=C(SCH_2\,CH_2CH_2CH_3)OR$ (R= $-CH_3$ and $-CH_2CH_3$) were prepared and fully characterized by spectroscopic methods, accounting for the feasibility of alkylation procedure for obtaining imidothiocarbonate with high selectivity.

ACKNOWLEDGMENTS

We thank financial support from CONICET (PIP 1529), ANPCYT (PME06 2804, PICT06 2315, and PICT 2130), and UNLP, Argentina. CODV, OEP, GAE, and MFE are research fellows of CONICET.

CONFLICT OF INTEREST STATEMENT

The authors declare that they have no conflict of interest.

SUPPORTING INFORMATION

a. Characterization of products (HSQC Figures S1a, b, ^{1}H NMR Figures S2a-f, ^{13}C NMR Figures S3a-f and FTIR spectra Figures S4a-f). b. Tables of experimental and calculated frequencies and intensities for **I** and **II** (Table S1a, b), fractional coordinates and equivalent isotropic displacement parameters of the non-H atoms (Tables S2a, b), full bond distances and angles (Tables S3a, b), atomic anisotropic displacement parameters (Table S4a, b), hydrogen atoms positions and isotropic displacement parameters (Table S5a, b), torsion angles (Tables S6a, b) and H-bond distances and angles (Tables S7a, b) discussed herein.

Table of contents

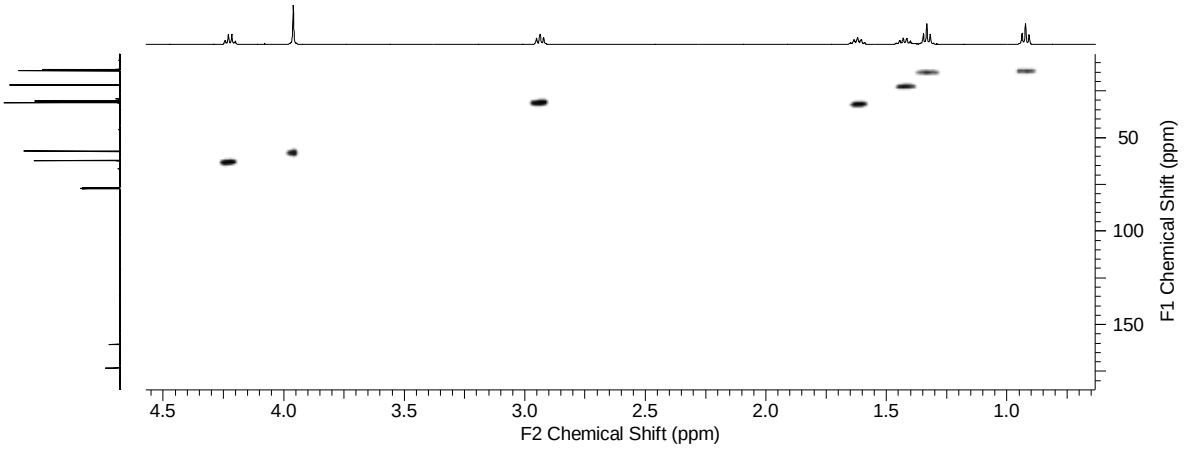

Figure S1a. 2D-NMR (HSQC) spectrum of **V**.

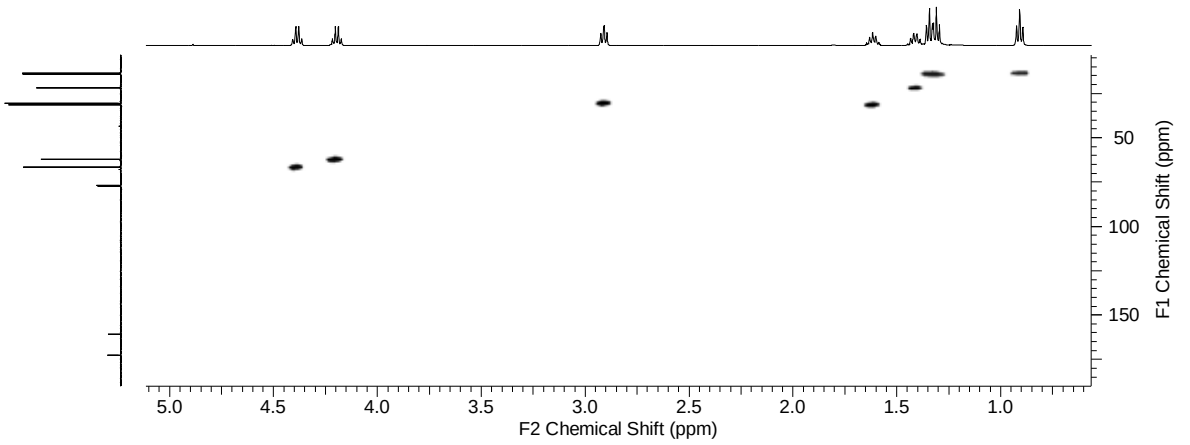

Figure S1b. 2D-NMR (HSQC) spectrum of **VI**.

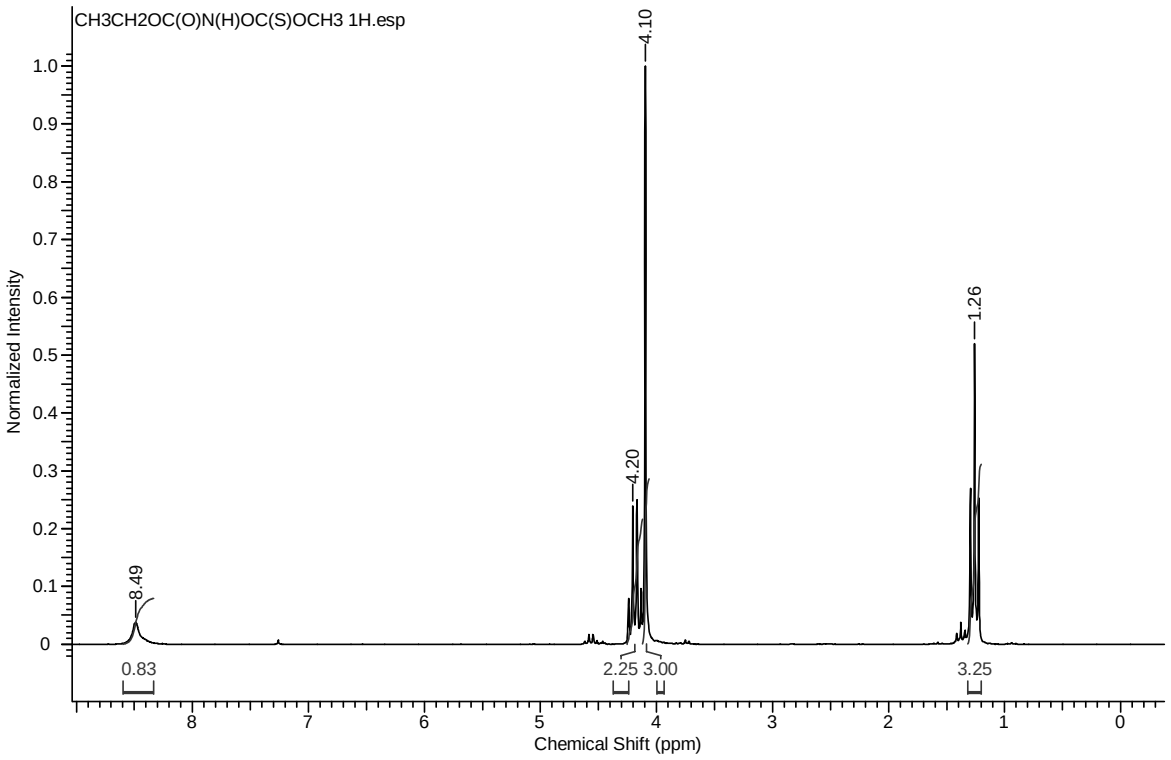

Figure S2a. ^{1}H NMR spectrum of **I**.

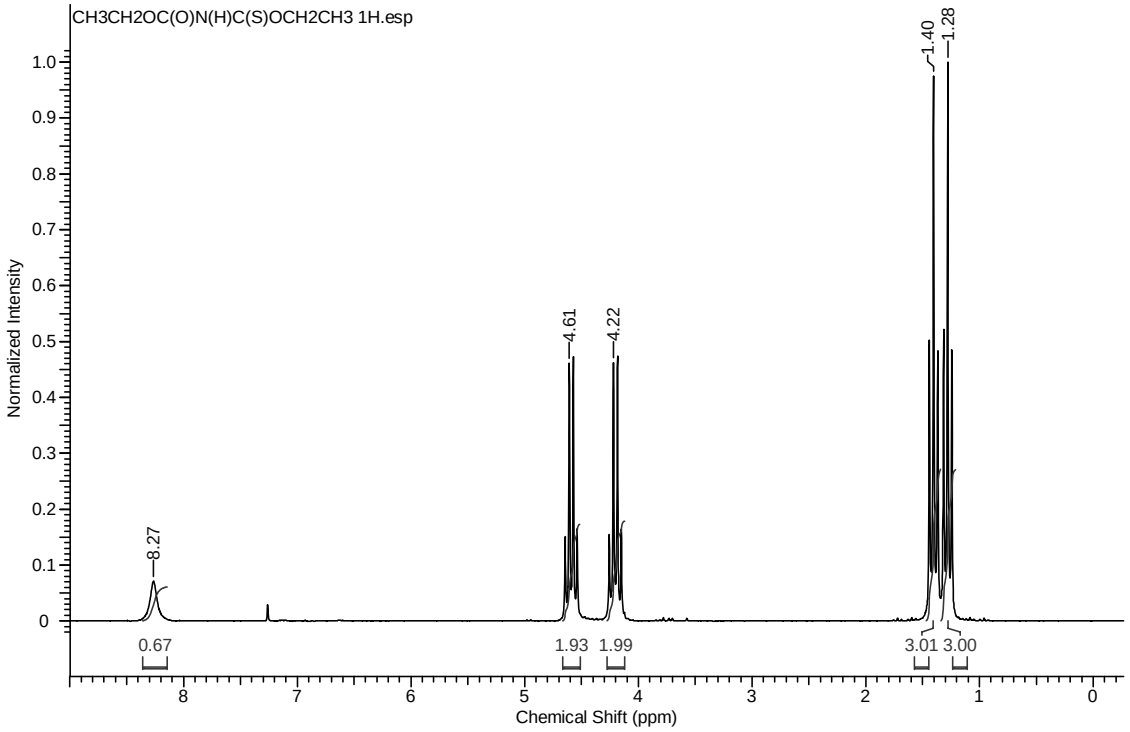

Figure S2b. ^{1}H NMR spectrum of **II**.

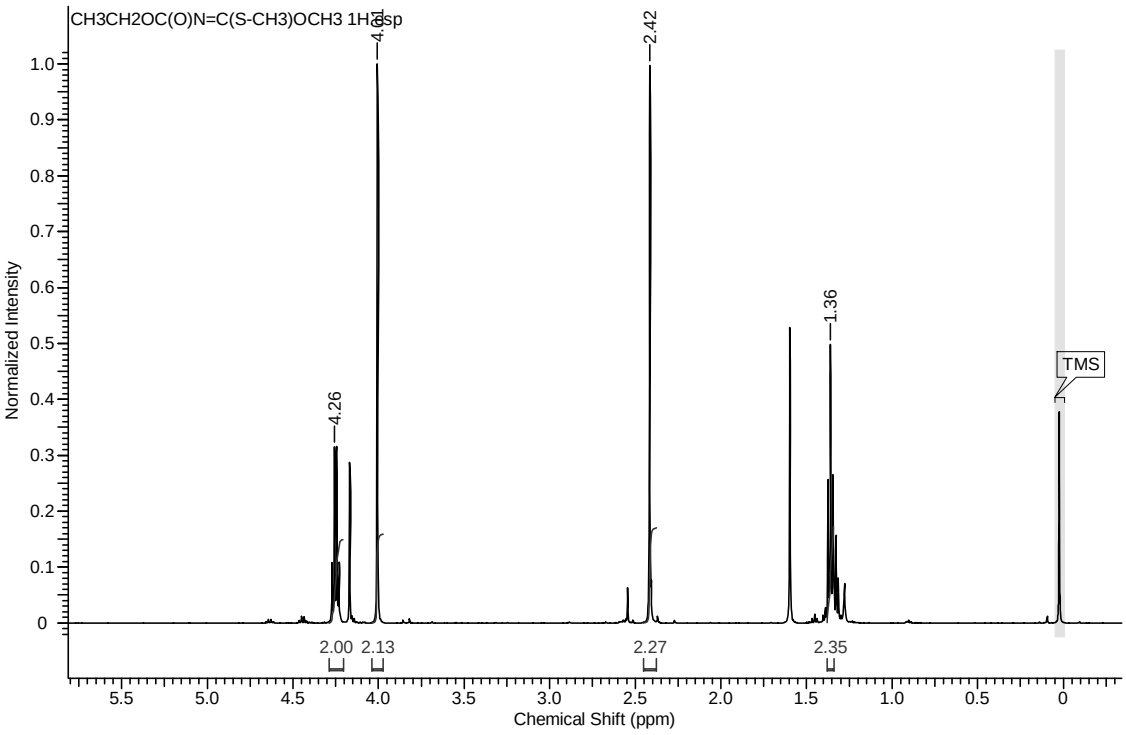

Figure S2c. ^{1}H NMR spectrum of **III**.

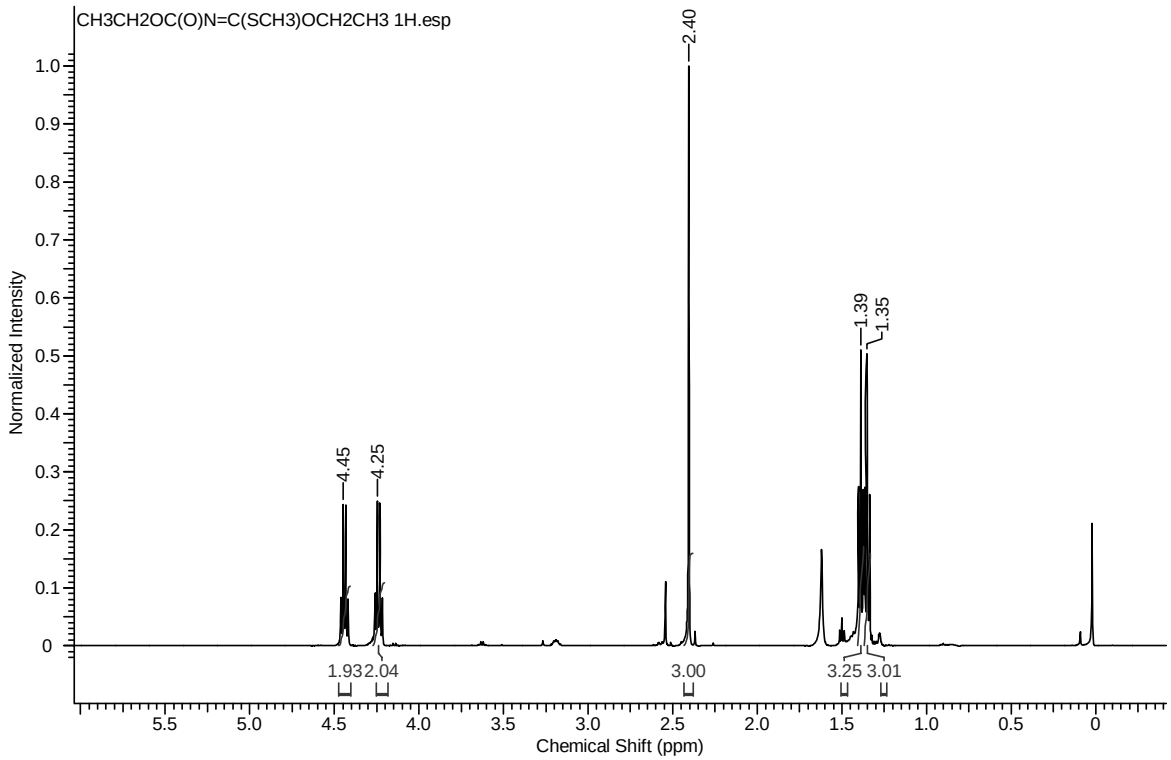

Figure S2d. ^{1}H NMR spectrum of **IV**.

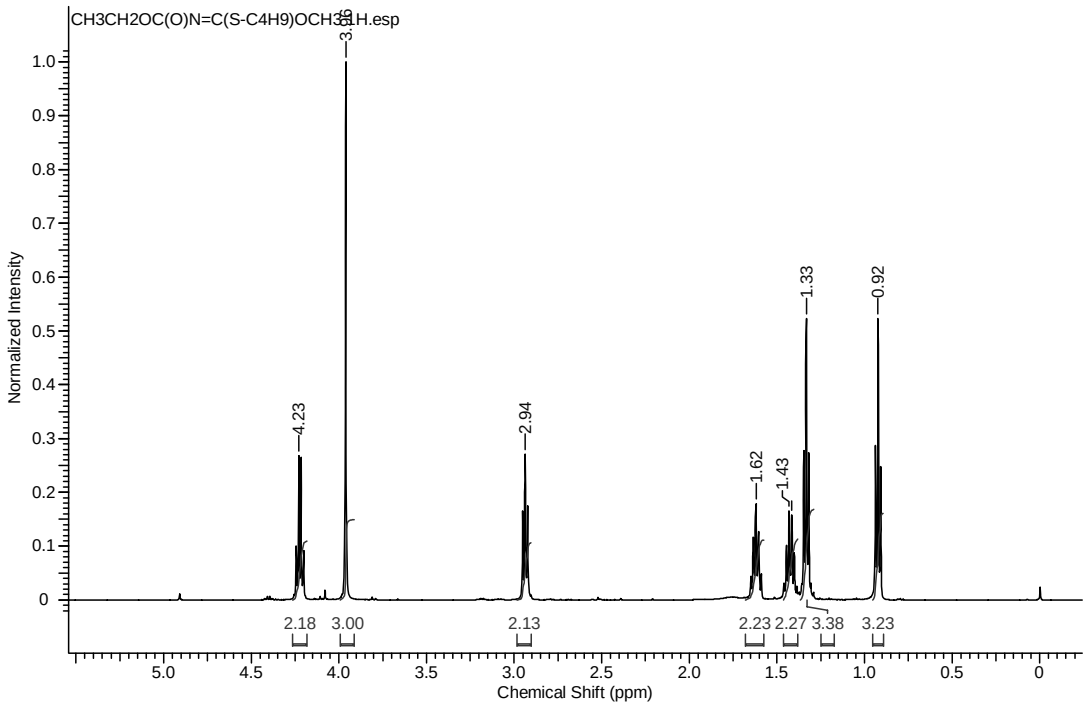

Figure S2e. ^{1}H NMR spectrum of **V**.

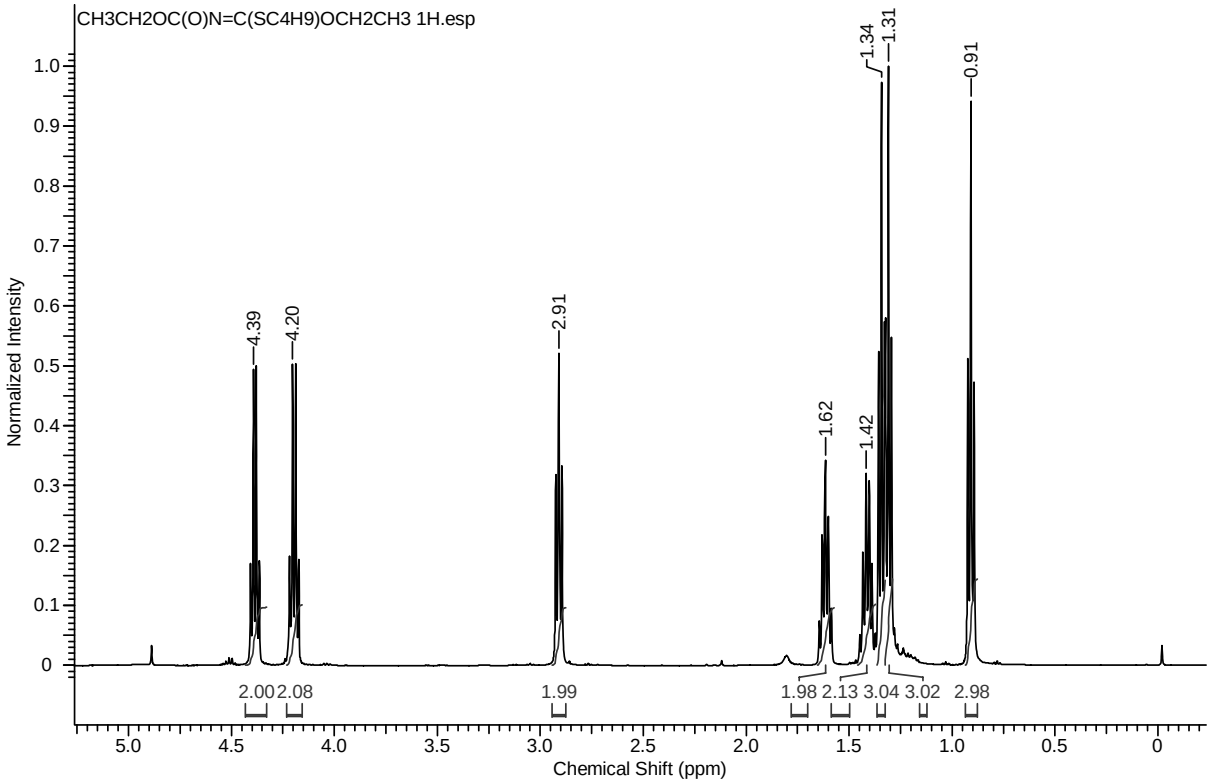

Figure S2f. ^{1}H NMR spectrum of **VI**.

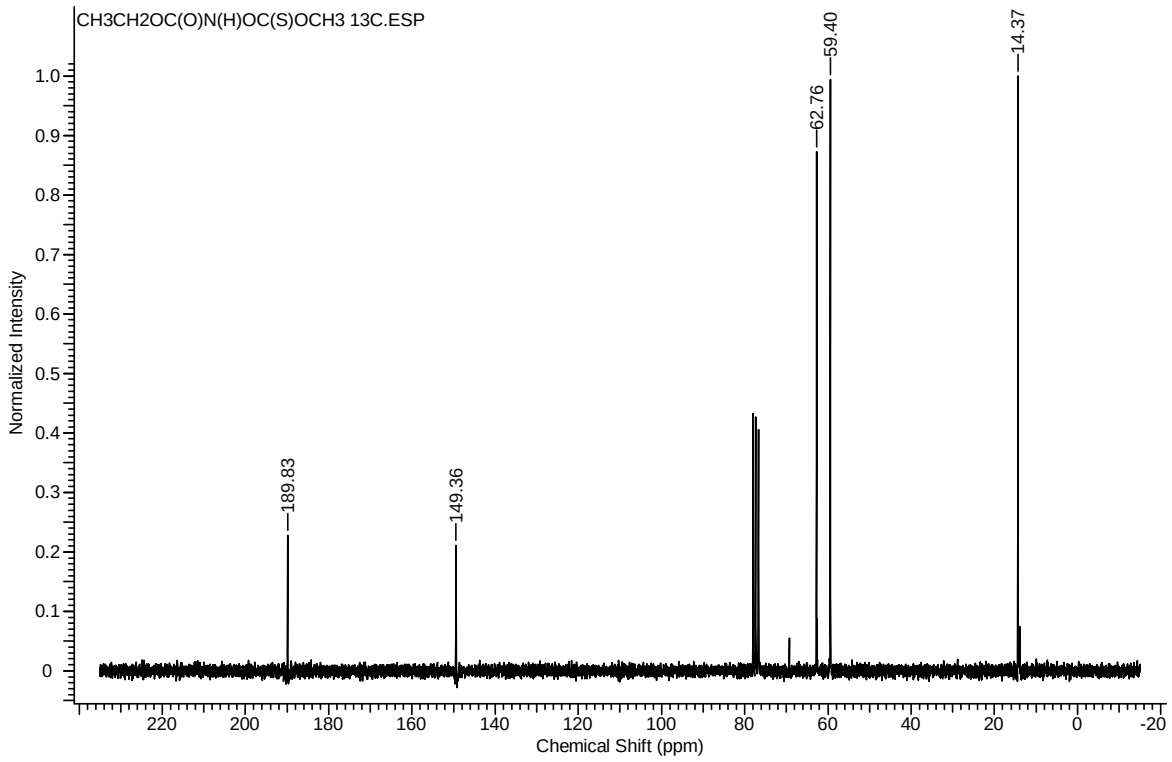

Figure S3a. ^{13}C NMR spectrum of **I**.

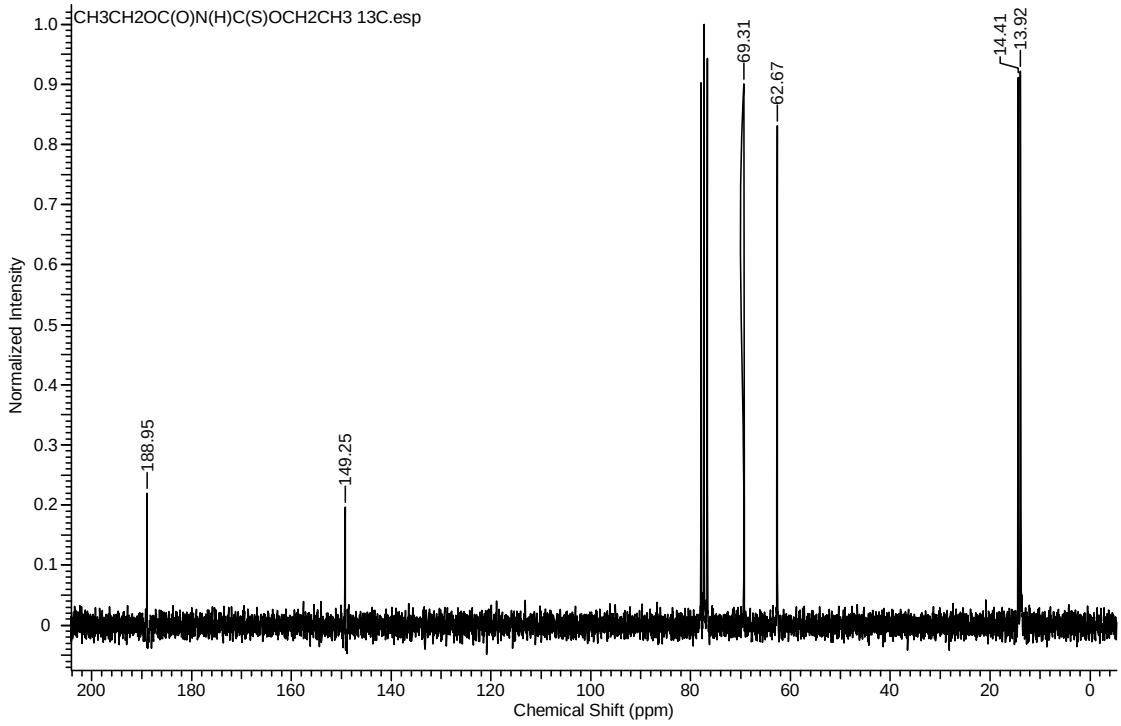

Figure S3b. ^{13}C NMR spectrum of **II**.

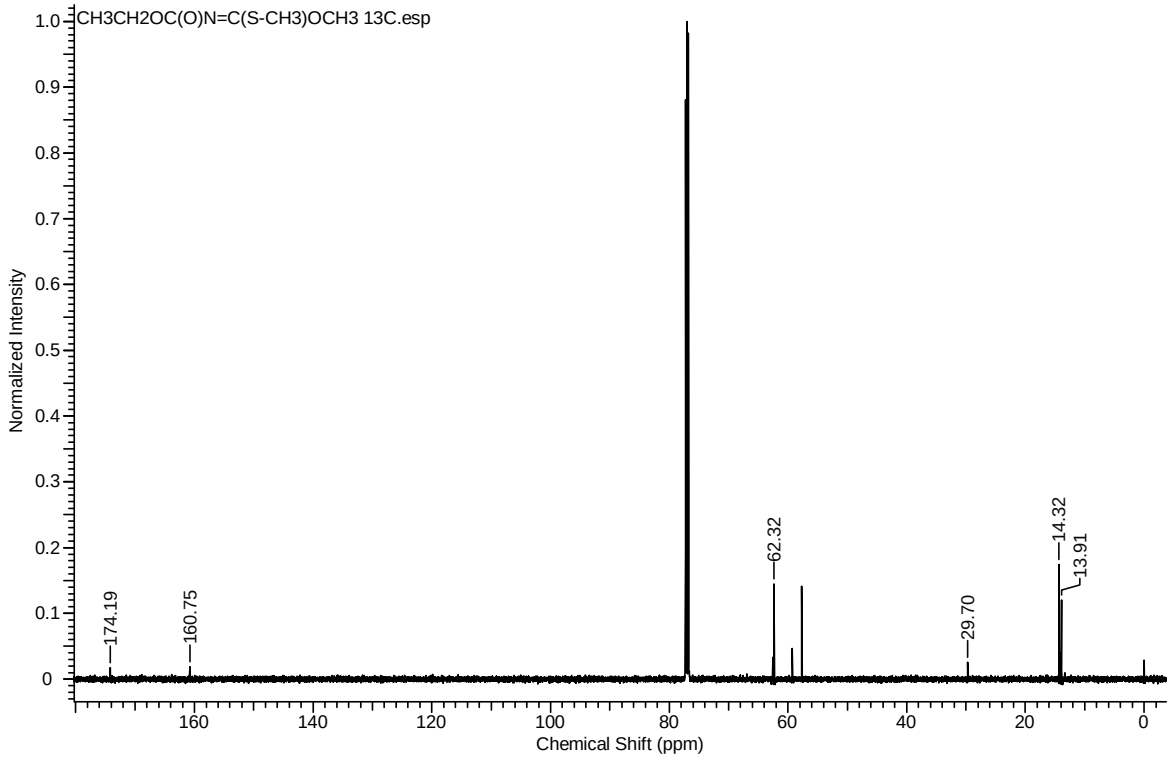

Figure S3c. ^{13}C NMR spectrum of **III**.

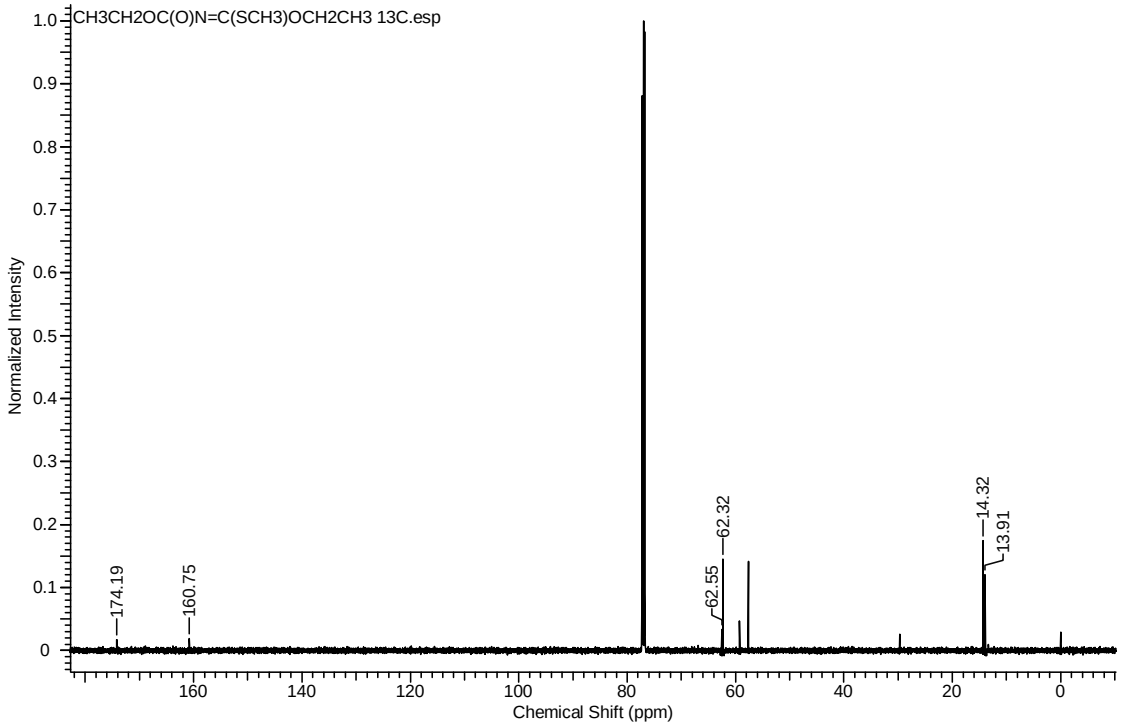

Figure S3d. ^{13}C NMR spectrum of **IV**.

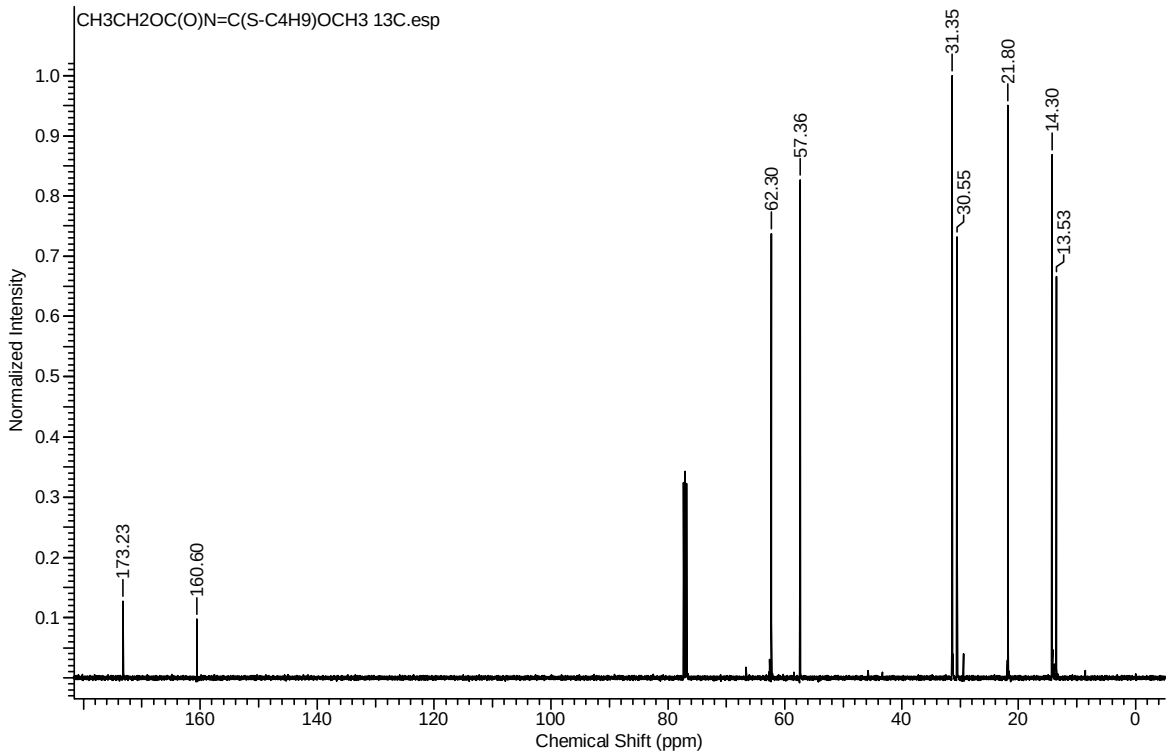

Figure S3e. ^{13}C NMR spectrum of **V**.

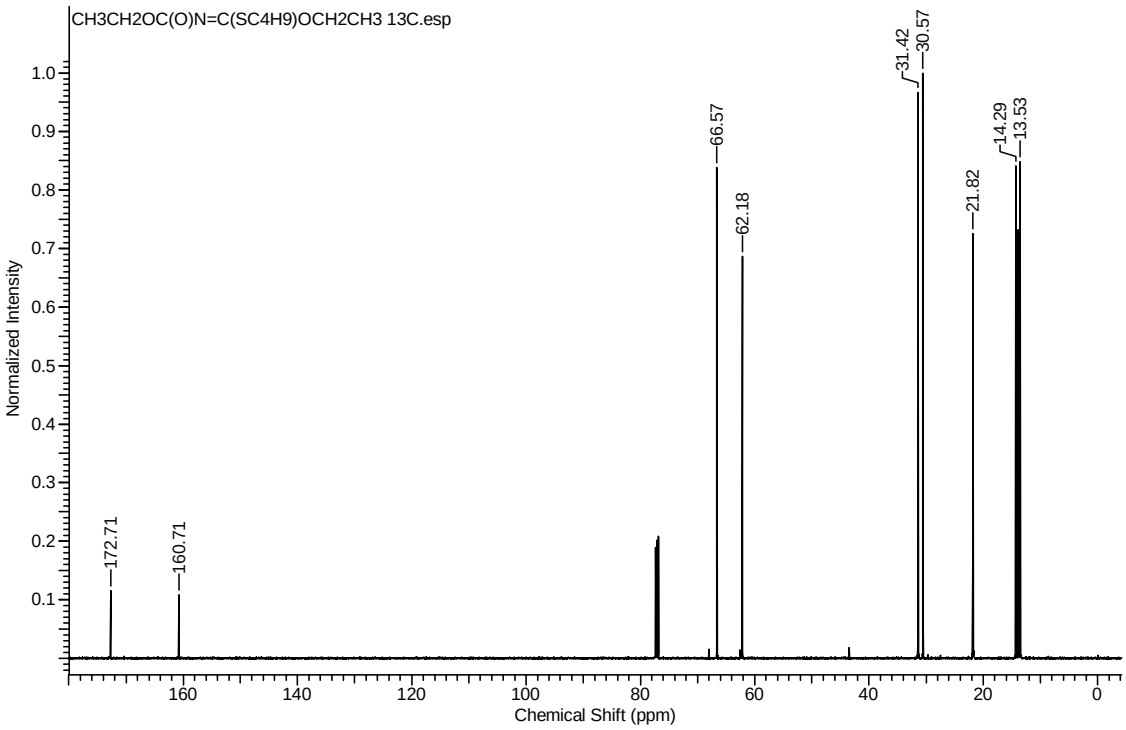

Figure S3f. ^{13}C NMR spectrum of **VI**.

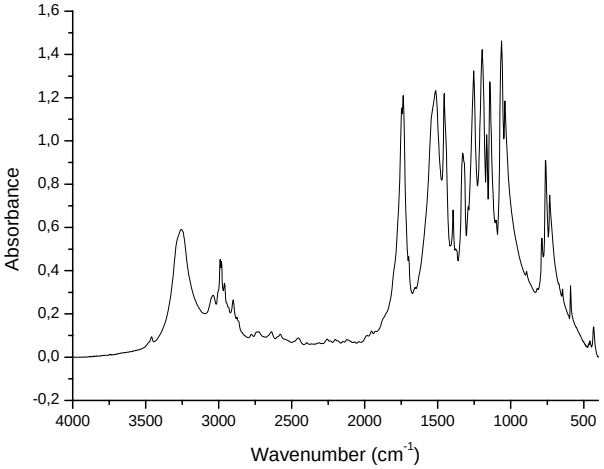

Figure S4a. FTIR spectrum of **I**.

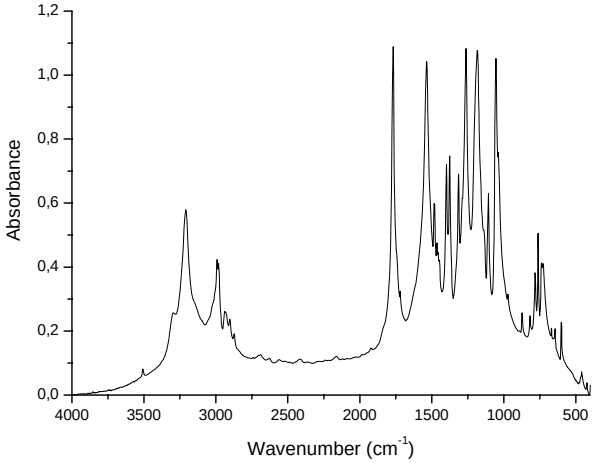

Figure S4b. FTIR spectrum of **II**.

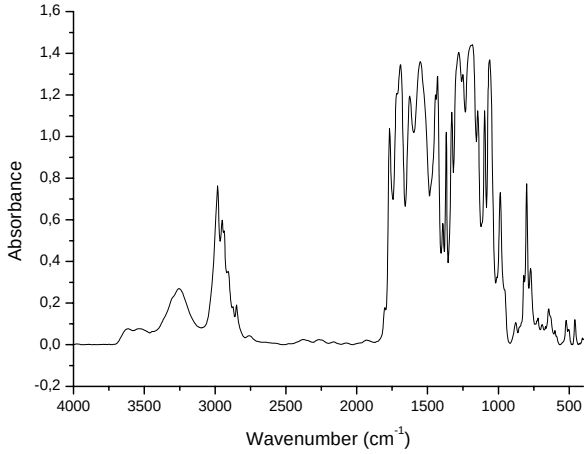

Figure S4c. FTIR spectrum of **III**.

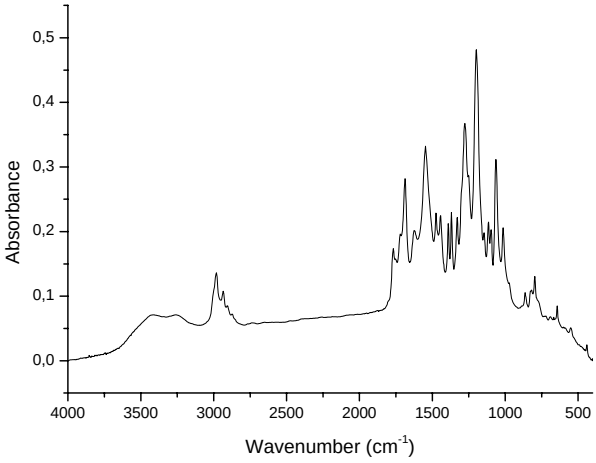

Figure S4d. FTIR spectrum of **IV**.

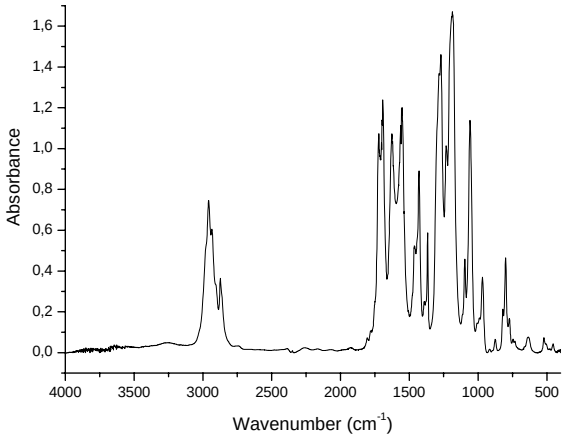

Figure S4e. FTIR spectrum of **V**.

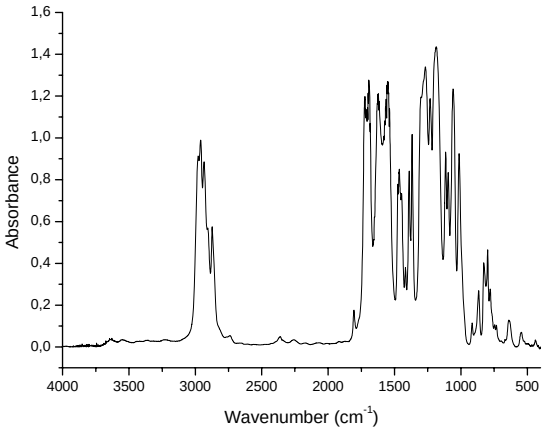

Figure S4f. FTIR spectrum of **VI.**

Table S1a. Experimental and calculated [B3LYP/6-311++G**] frequencies and intensities for **I**. Intensities: vs = very strong, s = strong, w = weak, vw = very weak, vvw = very very weak, sh = shoulder. For δ, ν, τ y δoop "bending", "stretching", "torsion angle" and the deformation "out-of-plane", respectively. [1-5]Carbon atom, counted in the direction from the neighboring ethyl to group C=O. (*: Proposed assignment.)

Experimental		**Calculated**	**Assignment*/Symmetry**
Mode	**IR**	**B3LYP/6-311++G****	
		anti-syn-anti	
	3458vw		
	3278sh		
ν_1	3258s	3623(9.8)	ν(NH)(100)/A'
ν_2	3042w	3163(1.7)	$\nu_d(C^5H_3)$ (92)/A"
ν_3	3006sh	3133(1.9)	$\nu_{as}(C^5H)$ (63)/A"
ν_4	2989s	3118(5.6)	$\nu_{as}(C^1H)$ (79) + $\nu_{as}(C^2H)$ (79)/A"
ν_5	2961s	3105(3.7)	$\nu_d(C^1H_3)$ (97)/A'
ν_6	2954sh	3091(<1)	$\nu_{as}(C^1H)$ (21) + $\nu_{as}(C^2H)$ (79)/A"
ν_7	2901w	3055(2.6)	$\nu_s(C^2H)$ (92)/A'
ν_8	2874vw	3054(3.5)	$\nu_s(C^5H_3)$ (97)/A'
ν_9	2863sh	3038(2.5)	$\nu_s(C^1H_3)$(99)/A'
ν_{10}	1742vs	1823(59)	ν(C=O)(85)/A'
ν_{11}	1514vs	1540(100)	δ(NH)(53) + δ(HNC)(15)/A'
ν_{12}		1519(6.6)	$\delta_s(HC^2H)$/A'
ν_{13}	1455vs	1498(<1)	$\delta_s(HC^1H)$/A'
ν_{14}	1448sh	1492(1.7)	$\delta_d(HC^5H)$/A'
ν_{15}	1394w	1486(1)	$\delta(C^1H_3)$/A"
ν_{16}		1479(2)	$\delta_s(C^5H_3)$ + $\delta(C^5H_3)$ + $\tau(HC^4OC^5)$(83)/A'
ν_{17}		1480(33)	$\delta(HC^5H)$/A"
ν_{18}	1373vvw	1427(4.3)	$\delta(C^5H_3)$/A'
ν_{19}		1397(<1)	$\tau(HCOC)^{1,2}$(66)/A'
ν_{20}	1328s	1348(48)	[$\nu(NC^4)$ + $\nu(OC^4)$](71)/A'
ν_{21}	1291vvw	1299(<1)	δ(HCO)(64) + [$\tau(HC^2OC^3)$ + $\tau(HC^1C^2O)$](19)/A"
ν_{22}	1255vs	1264(51)	δoop(C^5HOH) (11) + [$\nu(OC^3)$ + ν(CS)](44)/A'
ν_{23}	1195vs	1199(48)	[$\nu(OC^3)$ + ν(CS)](13) + δoop(C^5HOH) (40)/A'
ν_{24}		1178(<1)	δ(HCO)(33) + [$\tau(HC^2OC^3)$ + $\tau(HC^1C^2O)$](46)/A"
ν_{25}	1165s	1169(<1)	$\tau(HC^4OC^5)$, (16) + $\delta(HC^5O)$ (83)/A"
ν_{26}	1142s	1162(<1)	δ(N-H)(53) + δ(HNC)(15) + δoop(CHOH)(21)/A'
ν_{27}	1100w	1136(<1)	τ(HCCO)(41)/A'
ν_{28}	1063vs	1091(7.1)	[δ(CNC) + δ(NCO)](21)/A'
ν_{29}	1039vs	1054(9)	[$\nu(C^1$-$C^2)$ + ν(N-C(O)) + $\nu(O$-$C^2)$ + $\nu(O$-$C^5)$](55)/A'
ν_{30}	1004sh	1004(1.7)	[$\nu(C^1$-$C^2)$ + ν(N-C(O)) + $\nu(O$-$C^2)$ + ν(O-C(O))](60)/A'
ν_{31}	892vvw	899(<1)	[$\nu(O$-$C^2)$ + $\nu(O$-$C^5)$](43) + τ(HCCO)(16)/A'

Table S1a continued..

ν_{32}	821vvw	815(<1)	[τ(HC^{1}OC^2) + τ(HC^{1}C^{2}O)](77)/A”
ν_{33}	787w	793(<1)	[δ(CNC) + δ(NCO)](15) + [δ(COC) + δ(CCO) + δ(OCO)](11) + ν(OC^{3,5}) (52)/A’
ν_{34}	762s	771(3.5)	δoop(ONOC)/A”
ν_{35}	733w	747(1.3)	[ν(OC^3) + ν(CS)](22) + [ν(OC^5) + ν(CNC)](13) + [δ(COC) + δ(CCO) + δ(OCO)](45)/A’
ν_{36}	643w	650(9.8)	τ(HNCO)(97)/A”
ν_{37}	589w	634(<1)	δoop(SNOC)(94)/A”
ν_{38}	458vvw	593(<1)	[δ(C^{4}OC^5) + δ(OCS)](60) + [ν(OC^5) + ν(CS)](15)/A’
ν_{39}	432w	419(<1)	[δ(CCO) + δ(NCO)](66)/A’
ν_{40}		358(<1)	[δ(C^{4,2}O^{3,1}C^{5,3}) + δ(C^{1}C^{2}O) + δ(NC^{3,4}O^{1,3}) + δ(O^{1}CO^2)](72)/A’
ν_{41}		321(<1)	[δ(NCN) + δ(NCO^{3,1})](17) + [δ(CO^{3}C) + δ(O^{3}CS)](15) + [ν(O^{1,2}C^{2,5}) + ν(NC^3) + ν(C^{1}C^2)](10)/A’
ν_{42}		268(2)	δ(C^{3}NC^4)(75) + [δ(C^{4}OC^5) + δ(OCS)](79)/A’
ν_{43}		260(<1)	τ(HC^{1}C^{2}O)(89)/A”
ν_{44}		201(<1)	δ(C^{3}NC^4)(75) + [δ(C^{4}OC^5) + δ(OCS)](79)/A’
ν_{45}		197(<1)	τ(HC^{4}OC^5)(89) + τ(C^{4}NC^{5}O)(61)/A”
ν_{46}		161(<1)	τ(HC^{4}OC^5)(67) + δ(HCH)(75) + τ(C^{4}NC^{3}O)(24)/A”
ν_{47}		131(<1)	τ(C^{2,4}NC^{3,5}O)(86)/A”
ν_{48}		102(<1)	[δ(CNC) + δ(C^{2}OC^3) + δ(C^{1}C^{2}O) + δ(NC^{3}O)](90)/A’
ν_{49}		66(<1)	[τ(CNCO^1) + τ(C^{3}OC^{2}C^1) + τ(C^{2,4}OC^{3,5}N)](78)/A”
ν_{50}		52(<1)	[τ(CNCO^3) + τ(C^{3,5}OC^{2,4}C^{1,3})](83)/A”
ν_{51}		31(<1)	[τ(CNCO^3) + τ(C^{3}OC^{2}C^1)](82)/A”

Table S1b. Experimental and calculated [B3LYP/6-311++G**] frequencies and intensities for **II**. Intensities: vs = very strong, s = strong, w = weak, vw = very weak, vvw = very very weak, sh = shoulder. For δ, ν, τ y δoop “bending”, “stretching”, “torsion angle” and the deformation “out-of-plane”, respectively. [1-6]Carbon atom, counted in the direction from the neighboring ethyl to group C=O. * Proposed assignment.

Experimental		**Calculate**	**Assignment*/Symmetry**
Mode	**IR**	**B3LYP/6-311++G****	
		anti-syn-anti-anti	
	3507w		
	3295sh		
ν_1	3209vs	3621(9)	ν(NH)(100)/A’
ν_2	3021sh	3124(4)	ν_{as}(C^{5,6}H)(89)/A”
ν_3	3009sh	3118(5)	ν_{as}(C^{1,2}H)(96)/A”
ν_4	2993s	3108(3)	ν_d(C^{6}H$_3$)(92)/A’
ν_5	2981s	3105(3)	ν_d(C^{1}H$_3$)(97)/A’
ν_6		3098(<1)	ν_{as}(C^{5,6}H)(89)/A”

Table S1b continued..

ν_7		3092(<1)	$\nu_{as}(C^{1,2}H)(96)/A''$
ν_8	2939w	3058(<1)	$\nu_s(C^5H)(98)/A'$
ν_9	2928	3056(2)	$\nu_s(C^2H)(98)/A'$
ν_{10}	2903w	3041(2)	$\nu_s(C^6H_3)(94)/A'$
ν_{11}	2872w	3038(2)	$\nu_s(C^1H_3)(99)/A'$
ν_{12}	1770vs	1822(53)	$\nu(C=O)(85)/A'$
ν_{13}	1536vs	1536(88)	$\delta(HNC^3)(49) + \nu(NC^3)(13) + \delta(HC^2H)(14)/A'$
ν_{14}	1483m	1519(5)	$\delta(HC^{2,5}H)(42) + \delta(HC^5H)(17)/A'$
ν_{15}	1464m	1516(17)	$\delta(HC^5H)(53) + \tau(HC^4OC^5)(11)/A''$
ν_{16}	1456w	1499(<1)	$\tau(HC^1C^2O)(18) + \delta(HC^1H)(55)/A''$
ν_{17}	1446w	1496(<1)	$\tau(HC^5C^6O)(16) + \delta(HC^5H)(64)/A'$
ν_{18}		1486(1)	$\delta(HC^1H)(39) + \tau(HC^2OC^3)(16)/A''$
ν_{19}		1483(1)	$\delta(HC^6H)(38) + \tau(HC^5C^6O)(24) + \tau(HC^4OC^5)(10)/A''$
ν_{20}		1431(6)	$\delta(HC^6H)(38) + \tau(HC^4OC^5)(33)/A'$
ν_{21}		1426(4)	$\delta(HC^1H)(23) + \tau(HC^2OC^3)(26)/A'$
ν_{22}	1398s	1409(13)	$\nu(NC^4)(11) + \delta(HC^6H)(20) + \tau(HC^4OC^5)(22)/A''$
ν_{23}	1375s	1398(2)	$\delta(HC^2H)(13) + \tau(HC^2OC^3)(42)/A'$
ν_{24}	1314s	1331(47)	$\nu(NC^4)(53) + \tau(HC^4OC^5)(22)/A'$
ν_{25}	1288sh	1299(<1)	$\delta(HC^2O)(71) + \tau(HC^2OC^3)(18)/A''$
ν_{26}		1293(<1)	$\delta(HC^5C^6)(76)/A''$
ν_{27}	1262vs	1261(53)	$[\nu(OC^{3,4}) + \nu(CS)](57)/A'$
ν_{28}		1178(<1)	$\delta(HC^2O)(27) + \tau(HC^2OC^3)(39)/A''$
ν_{29}	1182vs	1176(100)	$\delta(NC^4)(57) + \delta(HNC)(21)/A'$
ν_{30}		1174(<1)	$\delta(HC^5C^6)(18) + \tau(HC^4OC^5)(57)/A''$
ν_{31}	1136sh	1135(<1)	$\tau(HC^1C^2O)(39) + \delta(HC^1H)(10)/A'$
ν_{32}	1107s	1127(8)	$\nu(C^5C^6)(23) + \tau(HC^5C^6O)(36)/A'$
ν_{33}	1052vs	1071(60)	$\nu(C^2O)(67)/A'$
ν_{34}	1039sh	1054(4)	$[\nu(C^1\text{-}C^2) + \nu(N\text{-}C(O)) + \nu(O^{2,3}\text{-}C^{3,5})](52)/A'$
ν_{35}		1003(2)	$[\nu(C^1\text{-}C^2) + \nu(N\text{-}C(O))](69)/A'$
ν_{36}	971w	978(<1)	$\nu(C^1\text{-}C^2)(35) + \tau(HC^5C^6O)(16)/A'$
ν_{37}	872w	884(<1)	$[\nu(C^1\text{-}C^2) + \nu(C^{2,3}O)](47) + \tau(HC^1C^2O)(17)/A'$
ν_{38}	817w	816(<1)	$[\tau(HC^1OC^2) + \tau(HC^2C^3O)](78)/A''$
ν_{39}		813(<1)	$\tau(HC^5C^6O)(77)/A''$
ν_{40}	761m	779(<1)	$\nu(OC^5)(43) + \delta(OC^3O)(10)/A'$
ν_{41}	738m	770(3)	$\delta oop(ONOC)/A''$
ν_{42}	727m	747(2)	$\nu(NC^4)(10) + \nu(OC^5)(21) + \delta(OC^3O)(45)/A'$
ν_{43}	668w	650(9)	$\tau(HNCO)(96)/A''$

Table S1b continued..

ν_{44}	646w	633(<1)	δoop(SNOC)(93)/A”
ν_{45}	600m	607(<1)	$\nu(C^2O)(10) + [\delta(C^4OC^5) + \delta(NC^3O) + \delta(OCS)](66)$/A’
ν_{46}	459vw	413(<1)	$[\delta(C^1C^2O) + \delta(NC^{3,4}O)](80)$/A’
ν_{47}	422vw	387(<1)	$\nu(C^5O)(12) + [\delta(C^{1,5}C^{2,6}O) + \delta(NC^4O) + \delta(CNC)](48)$/A’
ν_{48}		339(1)	$[\delta(C^4C^5O) + \delta(C^2OC^3) + \delta(NC^3O) + \delta(O^1CO^2)](68)$/A’
ν_{49}		295(<1)	$[\delta(NC^4O) + \delta(OC^4S) + \delta(CNC) + \delta(C^6C^5O)](49)$/A’
ν_{50}		259(<1)	$\tau(HC^1C^2O)(78)$/A”
ν_{51}		253(<1)	$\tau(HC^5C^6O)(76)$/A”
ν_{52}		242(2)	$[\delta(OC^4S) + \delta(CNC) + \delta(C^{2,4}OC^{3,5})](72)$/A’
ν_{53}		171(<1)	$\tau(HC^5C^6O)(12) + [\tau(C^{2,4}OC^{3,5}N) + \tau(C^3NC^4O^1) + \tau(C^4OC^5C^6)](73)$/A”
ν_{54}		153(<1)	$[\delta(C^1C^2O) + \delta(C^2OC^3) + \delta(NC^{3,4}O)](74)$/A’
ν_{55}		124(<1)	$\tau(C^{2,4}OC^{3,5}N)(86)$/A”
ν_{56}		81(<1)	$[\delta(CNC) + \delta(C^{2,4}OC^{3,5}) + \delta(NCO^{1,3})](84)$/A’
ν_{57}		72(<1)	$[\tau(CNCO^1) + \tau(C^{3,4}OC^{2,5}C^{1,6}) + \tau(C^{2,4}OC^{3,5}N)](73)$/A”
ν_{58}		65(<1)	$\tau(C^{1,4}OC^{2,5}C^{3,6})(71)$/A”
ν_{59}		49(<1)	$[\tau(CNCO^1) + \tau(C^3OC^2C^1)](80)$/A”
ν_{60}		32(<1)	$[\tau(CNCO^1) + \tau(C^{1,4}OC^{2,5}C^{3,6})](83)$/A”

Crystallographic Supporting Information

Table S2a. Atomic coordinates (x 104) and equivalent isotropic displacement parameters (Å2x 103) for (I). U(eq) is defined as one third of the trace of the orthogonalized Uij tensor.

Atom	x	y	z	(eq)
C(1)	-5707(6)	12604(1)	4461(3)	43(1)
C(2)	-6015(5)	12225(1)	5782(2)	37(1)
C(3)	-4399(5)	11092(1)	6747(2)	29(1)
C(4)	-1973(5)	9881(1)	7189(2)	29(1)
C(5)	-2487(6)	9276(1)	9269(2)	39(1)
N(1)	-2669(4)	10486(1)	6437(2)	29(1)
O(1)	-5996(4)	11162(1)	7674(2)	39(1)
O(2)	-4031(3)	11585(1)	5787(1)	33(1)
O(3)	-3010(4)	9906(1)	8403(1)	34(1)
S(1)	30(1)	9203(1)	6594(1)	34(1)

Table S2b. Atomic coordinates (x 104) and equivalent isotropic displacement parameters (Å2 x 103) for (II). U(eq) is defined as one third of the trace of the orthogonalized Uij tensor.

Atom	x	y	z	U(eq)
C(1)	-7232(11)	1875(4)	712(4)	43(1)
C(2)	-4989(9)	3399(4)	778(3)	34(1)
C(3)	-776(8)	5156(4)	2161(3)	30(1)
C(4)	3182(8)	6662(3)	3936(3)	29(1)
C(5)	7155(8)	8841(4)	3748(3)	32(1)
C(6)	8446(11)	9489(5)	2758(4)	42(1)
O(1)	-125(6)	5946(3)	1459(2)	38(1)
O(2)	-3032(6)	3840(3)	1957(2)	36(1)
O(3)	4645(6)	7460(2)	3230(2)	33(1)
N(1)	700(7)	5459(3)	3341(2)	32(1)
S(1)	4142(2)	6998(1)	5373(1)	35(1)

Table S3a. Bond lengths [Å] and angles [°] for(I).

C(1)-C(2)	1.499(3)
C(2)-O(2)	1.453(3)
C(3)-O(1)	1.200(2)
C(3)-O(2)	1.335(2)
C(3)-N(1)	1.392(3)
C(4)-O(3)	1.320(2)
C(4)-N(1)	1.359(3)
C(4)-S(1)	1.657(2)
C(5)-O(3)	1.449(3)
O(2)-C(2)-C(1)	106.38(18)
O(1)-C(3)-O(2)	125.77(18)
O(1)-C(3)-N(1)	127.32(18)
O(2)-C(3)-N(1)	106.88(16)
O(3)-C(4)-N(1)	113.19(17)
O(3)-C(4)-S(1)	125.46(15)
N(1)-C(4)-S(1)	121.35(14)
C(4)-N(1)-C(3)	129.29(17)
C(3)-O(2)-C(2)	116.62(16)
C(4)-O(3)-C(5)	117.54(17)

Table S3b. Bond lengths [Å] and angles [°] for (II).

C(1)-C(2)	1.500(5)
C(2)-O(2)	1.458(4)
C(3)-O(1)	1.203(4)
C(3)-O(2)	1.336(4)
C(3)-N(1)	1.399(4)
C(4)-O(3)	1.321(4)
C(4)-N(1)	1.368(4)
C(4)-S(1)	1.651(3)
C(5)-O(3)	1.455(4)
C(5)-C(6)	1.505(5)
O(2)-C(2)-C(1)	106.8(3)
O(1)-C(3)-O(2)	126.3(3)
O(1)-C(3)-N(1)	125.9(3)
O(2)-C(3)-N(1)	107.8(3)
O(3)-C(4)-N(1)	112.2(3)

Table S3b continued..

O(3)-C(4)-S(1)	126.2(2)
N(1)-C(4)-S(1)	121.6(2)
O(3)-C(5)-C(6)	106.7(3)
C(3)-O(2)-C(2)	115.1(2)
C(4)-O(3)-C(5)	118.0(3)
C(4)-N(1)-C(3)	128.5(3)

Table S4a. Anisotropic displacement parameters (Å2 x 103) for (I). The anisotropic displacement factor exponent takes the form: -2π2[h2a*2U11 + ... + 2 h k a* b* U12].

Atom	**U11**	**U22**	**U33**	**U23**	**U13**	**U12**
C(1)	54(1)	31(1)	42(1)	5(1)	1(1)	-1(1)
C(2)	41(1)	30(1)	41(1)	3(1)	7(1)	3(1)
C(3)	34(1)	28(1)	26(1)	-1(1)	5(1)	-3(1)
C(4)	33(1)	30(1)	25(1)	-1(1)	7(1)	-5(1)
C(5)	54(1)	38(1)	28(1)	8(1)	14(1)	6(1)
N(1)	39(1)	28(1)	23(1)	1(1)	12(1)	1(1)
O(1)	53(1)	34(1)	32(1)	1(1)	19(1)	6(1)
O(2)	40(1)	30(1)	32(1)	5(1)	10(1)	4(1)
O(3)	48(1)	32(1)	24(1)	3(1)	13(1)	5(1)
S(1)	45(1)	29(1)	30(1)	1(1)	14(1)	4(1)

Table S4b. Anisotropic displacement parameters (Å2x 103) for (II). The anisotropic displacement factor exponent takes the form: -2π2[h2a*2U11 + ... + 2 h k a* b* U12].

Atom	**U11**	**U22**	**U33**	**U23**	**U13**	**U12**
C(1)	52(2)	37(2)	35(2)	9(2)	0(2)	1(2)
C(2)	43(2)	34(2)	22(2)	8(1)	1(1)	6(2)
C(3)	35(2)	28(2)	25(2)	5(1)	3(1)	8(1)
C(4)	33(2)	25(1)	29(2)	3(1)	3(1)	8(1)
C(5)	34(2)	29(2)	31(2)	5(1)	4(1)	2(1)
C(6)	44(2)	40(2)	41(2)	15(2)	10(2)	5(2)
O(1)	48(1)	36(1)	25(1)	12(1)	3(1)	2(1)
O(2)	47(1)	33(1)	25(1)	10(1)	2(1)	1(1)
O(3)	41(1)	31(1)	24(1)	6(1)	5(1)	3(1)
N(1)	40(2)	28(1)	24(1)	7(1)	2(1)	-1(1)
S(1)	45(1)	34(1)	23(1)	7(1)	2(1)	5(1)

Table S5a. Hydrogen coordinates (x 104) and isotropic displacement parameters (Å2x 103) for (I).

Atom	x	y	z	U(eq)
H(1)	-1920(70)	10510(16)	5690(30)	55(8)
H(1A)	-7030(70)	13025(16)	4430(30)	62(9)
H(1B)	-3530(70)	12739(15)	4430(30)	48(7)
H(1C)	-6330(70)	12305(16)	3690(30)	51(8)
H(2A)	-8120(70)	12059(16)	5810(30)	54(8)
H(2B)	-5260(70)	12514(18)	6520(30)	55(9)
H(5A)	-3370(60)	9363(14)	10050(30)	49(8)
H(5B)	-3620(70)	8888(17)	8860(30)	49(8)
H(5C)	-270(80)	9172(17)	9480(30)	57(9)

Table S5b. Hydrogen coordinates (x 104) and isotropic displacement parameters (Å2 x 103) for (II).

Atom	x	y	z	U(eq)
H(1)	-310(110)	4840(50)	3690(40)	50(12)
H(1A)	-8710(110)	1540(50)	-90(40)	57(13)
H(1B)	-6070(110)	1080(50)	810(40)	62(14)
H(1C)	-8760(110)	1800(50)	1310(40)	55(13)
H(2A)	-6190(90)	4120(40)	620(30)	32(9)
H(2B)	-3510(100)	3420(40)	180(40)	46(11)
H(5A)	9040(90)	8630(40)	4300(30)	31(9)
H(5B)	5990(100)	9480(50)	4240(40)	51(12)
H(6A)	6730(110)	9700(50)	2280(40)	48(12)
H(6B)	10140(130)	10450(60)	3080(50)	78(16)
H(6C)	9490(120)	8840(50)	2310(40)	63(14)

Table S6a. Torsion angles [°] for (I).

O(3)-C(4)-N(1)-C(3)	-3.2(3)
S(1)-C(4)-N(1)-C(3)	177.63(16)
O(1)-C(3)-N(1)-C(4)	-10.9(4)
O(2)-C(3)-N(1)-C(4)	170.87(19)
O(1)-C(3)-O(2)-C(2)	-7.3(3)
N(1)-C(3)-O(2)-C(2)	170.92(17)
C(1)-C(2)-O(2)-C(3)	-167.68(18)
N(1)-C(4)-O(3)-C(5)	177.85(19)
S(1)-C(4)-O(3)-C(5)	-3.0(3)

Table S6b. Torsion angles [°] for (II).

O(1)-C(3)-O(2)-C(2)	-4.0(5)
N(1)-C(3)-O(2)-C(2)	175.8(3)
C(1)-C(2)-O(2)-C(3)	177.4(3)
N(1)-C(4)-O(3)-C(5)	175.2(3)
S(1)-C(4)-O(3)-C(5)	-5.6(4)
C(6)-C(5)-O(3)-C(4)	178.6(3)
O(3)-C(4)-N(1)-C(3)	-12.3(5)
S(1)-C(4)-N(1)-C(3)	168.5(3)
O(1)-C(3)-N(1)-C(4)	-1.6(6)
O(2)-C(3)-N(1)-C(4)	178.5(3)

Table S7a. Hydrogen bonds for (I) [Å and °].

D-H...A	d(D-H)	d(H...A)	d(D...A)	<(DHA)
N(1)-H(1)...S(1)#1	0.83(3)	2.53(3)	3.352(2)	170(3)
C(5)-H(5A)...O(1)#2	0.91(3)	2.49(3)	3.254(3)	142(2)
C(5)-H(5A)...O(3)#2	0.91(3)	2.64(3)	3.482(3)	154(2)

Symmetry transformations used to generate equivalent atoms: #1 -x,-y+2, -z+1, #2 -x-1,-y+2,-z+2.

Table S7b. Hydrogen bonds for (II) [Å and °].

D-H...A	d(D-H)	d(H...A)	d(D...A)	<(DHA)
N(1)-H(1)...S(1)#1	0.83(5)	2.57(5)	3.389(3)	172(4)

Symmetry transformations used to generate equivalent atoms: #1 -x,-y+1,-z+1.

REFERENCES

1. Barany, G., Britton, D., Chen, L., Robert, P., Hammer, R. P., Henley, M. J., Schrader, A. M. and Young, Jr. V. G. 2015, J. Org. Chem. 80, 11313-11321.
2. Nagano, M., Matsui, T., Tobitsuka, J. and Oyamada, K. 1972, Chem. Pharm. Bull., 20, 2626.
3. Oyamada, K., Tobitzuca, J., Matsui, T. and Nagano, M. 1976, J. Agric. Chem. Soc. Japan, 50, 23.
4. Hope, G. A., Woods, R., Boyd, S. E. and Watling, K. 2004, Colloids Surf. A, 232, 129.
5. Woods, R. and Hope, G. A. 1999, Colloids Surf. A, 146, 63.
6. Torrico Vallejos, S., Erben, M. F., Piro, O. E., Castellano, E. E. and Della Védova, C. O. 2009, Polyhedron, 28, 937.
7. Atkins, P. R., Glue, S. E. J. and Kay, I. T. 1973, J. Chem. Soc. Perkin I, 2644.
8. Insuasty, H., Castro, E., Sánchez, E., Cobo, J. and Glidewell, C. 2010, Acta Cryst. C66, o141.
9. Kulkarni, S. V. 2000, US Patent 6066754.
10. Martínez-Álvarez, R., Martín, N. and Seoane, C. 2002, Eur. J. Mass Spectrom., 8, 367.
11. Agilent, 2014, CrysAlis PRO, Agilent Technologies Ltd., Yarnton, Oxfordshire, England.
12. Sheldrick, G. 2008, Acta Crystallogr. Sect. A, 64, 112.
13. Frisch, M. J., Trucks, G. W., Schlegel, H. B., Scuseria, G. E., Robb, M. A., Cheeseman, J. R., Montgomery, Jr., J. A., Vreven, T., Kudin, K. N., Burant, J. C., Millam, J. M., Iyengar, S. S., Tomasi, J., Barone, V., Mennucci, B., Cossi, M., Scalmani, G., Rega, N., Petersson, G. A., Nakatsuji, H., Hada, M., Ehara, M., Toyota, K., Fukuda, R., Hasegawa, J., Ishida, M., Nakajima, T., Honda, Y., Kitao, O., Nakai, H., Klene, M., Li, X., Knox, J. E., Hratchian, H. P., Cross, J. B., Bakken, V., Adamo, C., Jaramillo, J., Gomperts, R., Stratmann, R. E., Yazyev, O., Austin, A. J., Cammi, R., Pomelli, C., Ochterski, J. W., Ayala, P. Y., Morokuma, K., Voth, G. A., Salvador, P., Dannenberg, J. J., Zakrzewski, V. G., Dapprich, S., Daniels, A. D., Strain, M. C., Farkas, O., Malick, D. K., Rabuck, A. D., Raghavachari, K., Foresman, J. B., Ortiz, J. V., Cui, Q., Baboul, A. G., Clifford, S., Cioslowski, J., Stefanov, B. B., Liu, G., Liashenko, A., Piskorz, P., Komaromi, I., Martin, R. L., Fox, D. J., Keith, T., Al-Laham, M. A., Peng, C. Y., Nanayakkara, A., Challacombe, M., Gill, P. M. W., Johnson, B., Chen, W., Wong, M. W., Gonzalez, C. and Pople, J. A. 2004, GAUSSIAN 03, Revision C.02, Gaussian, Inc., Wallingford CT.

14. Arslan, H., Florke, U. and Külcü, N. 2007, Spectrochim. Acta, 67A.
15. Goerdeler, J. and Schulze, A. 1982, Chem. Ber., 115, 1252.
16. Tadbuppa, P. P. and Tiekink, E. R. 2007, Acta Crystallogr. Sect. E, 63, o1779.
17. Dillen, J., Woldu, M. G. and Koch, K. R. 2006, Acta Crystallogr. Sect. E, 62, o5225.
18. Dillen, J., Woldu, M. G. and Koche, K. R. 2006, Acta Crystallogr. Sect. E, 62, o5228.
19. Henley, M. J., Schrader, A. M., Young, Jr. V. G. and Barany, G. 2015, Acta Crystallogr. Sect. E, 71, o782.
20. Overberger, C. G. and Friedman, H. A. 1965, J. Polym. Sci., A3, 3625.
21. Torrico Vallejos, S., Erben, M. F., Willner, H., Boese, R. and Della Védova, C. O. 2007, J. Org. Chem., 72, 9074.
22. Torrico Vallejos, S., Erben, M. F., Boese, R., Piro, O. E., Castellano, E. E. and Della Védova, C. O. 2009, J. Mol. Struct., 918, 146.
23. Dillen, J., Woldu, M. G. and Koch, K. R. 2006, Acta Crystallogr. Sect. E, 62, o4819.
24. Johnson, C. K. 1976, ORTEP-II: a FORTRAN Thermal-Ellipsoid Plot Program for Crystal Structure Illustrations.
25. Allen, F. H., Kennard, O. and Watson, D. G. 1987, J. Chem. Soc. Perkin Trans., 11, S1-S19.
26. Allen, F. H., Kennard, O., Watson, D. G., Brammer, L., Orpen, A. G. and Taylor, R. 1987, J. Chem. Soc. Perkin Trans., 2, S1-S19.
27. Low, J. N., Cobo, J., Insuasty, H., Estrada, M., Cortés, E. and Glidewelld, C. 2004, Acta Cryst., C60, o483.
28. Benson, R. E., Broker, G. A., Daniels, L. M., Tiekink, E. R. T., Wardell, J. L. and Young, D. J. 2006, Acta Crystallogr. Sect. E, 62, o4106-o4108.
29. Saeed, A. and Floerke, U. 2006, Acta Crystallogr. Sect. E, 62, o2924.
30. Stockmann, S., Bruce, J., Miller, J. and Koch, K. R. 2008, Acta Crystallogr. Sect. C, 64, o166-o170.
31. Morales, A. D., Novoa de Armas, H., Blaton, N. M., Peeters, O. M., De Ranter, C. J., Márquez, H. and Pomés Hernández, R. 2000, Acta Crystallogr. Sect. C, 56, 1042.
32. Blewett, G., Esterhuysen, C., Bredenkamp, M. W. and Koch, K. R. 2004, Acta Crystallogr. C, 60, o862.
33. Morales, A. D., Novoa de Armas, H., Blaton, N. M., Peeters, O. M., De Ranter, C. J., Márquez, H. and Pomés Hernández, R. 2000, Acta Crystallogr. Sect. C, 56, 503.
34. Blewett, G., Bredenkamp, M. and Koch, K. R. 2005, Acta Crystallogr. C, 61, o469-72.
35. Jones, G. I. L., Lister, D. G., Owen, N. L., Gerry, M. C. L. and Palmieri, P. 1976, J. Mol. Spectrosc., 60, 348-360.
36. Wiberg, K. B. and Rablen, P. R. 1995, J. Am. Chem. Soc., 117, 2201-2209.